Supplemental Material for

High-throughput screening discovers anti-fibrotic properties of Haloperidol by hindering myofibroblast activation

Michael Rehman[1], Simone Vodret[1], Luca Braga[2], Corrado Guarnaccia[3], Fulvio Celsi[4], Giulia Rossetti[5], Valentina Martinelli[2], Tiziana Battini[1], Carlin Long[2], Kristina Vukusic[1], Tea Kocijan[1], Chiara Collesi[2,6], Nadja Ring[1], Natasa Skoko[3], Mauro Giacca[2,6], Giannino Del Sal[7,8], Marco Confalonieri[6], Marcello Raspa[9], Alessandro Marcello[10], Michael P. Myers[11], Sergio Crovella[3], Paolo Carloni[5], Serena Zacchigna[1,6]

[1]Cardiovascular Biology, [2]Molecular Medicine, [3]Biotechnology Development, [10]Molecular Virology, and [11]Protein Networks Laboratories, International Centre for Genetic Engineering and Biotechnology (ICGEB), Padriciano, 34149, Trieste, Italy
[4]Institute for Maternal and Child Health, IRCCS "Burlo Garofolo", Trieste, Italy
[5]Computational Biomedicine Section, Institute of Advanced Simulation IAS-5 and Institute of Neuroscience and Medicine INM-9, Forschungszentrum Jülich GmbH, 52425, Jülich, Germany
[6]Department of Medical, Surgical and Health Sciences, University of Trieste, 34149 Trieste, Italy
[7]National Laboratory CIB, Area Science Park Padriciano, Trieste, 34149, Italy
[8]Department of Life Sciences, University of Trieste, Trieste, 34127, Italy
[9]Consiglio Nazionale delle Ricerche (IBCN), CNR-Campus International Development (EMMA-INFRAFRONTIER-IMPC), Rome, Italy

This PDF file includes:

Supplementary Methods

Cell culture

Primary murine fibroblasts were isolated from skin, lung, kidney and hearts of adult CD1, C57BL/6 or αSMA-RFP/COLL-EGFP mice (1) by mechanical and enzymatic tissue digestion. Briefly, tissue was chopped in small chunks that were digested using a mixture of enzymes (Miltenyi Biotec, 130-098-305) for 1 hour at 37°C with mechanical dissociation followed by filtration through a 70 μm cell strainer and centrifugation. Fibroblasts were seeded on culture plates, changing the medium after 2 hours and never kept in culture for more than 3 passages. Primary human dermal fibroblasts and NIH3T3 were obtained from Lonza and ATCC, respectively. The lung adenocarcinoma cell line LG1233 was derived from lung tumors of C57BL/6 KP mice (K-rasLSL-G12D/+;p53fl/fl mice) and was kindly provided by Dr. Tyler Jacks (Massachusetts Institute of Technology, Cambridge, MA) (2). All cells were maintained in Dulbecco's Modified Eagle's Medium (DMEM), supplemented with 10% FBS. Myofibroblast differentiation was induced by TGFβ (25 ng/mL, Peprotech Inc, Cat. No. 100 35-B). Haloperidol (Haldol) was purchased from Janssen Pharmaceuticals, Nintedanib (Ofev) was purchased from Boehringer Ingelheim, and Pirfenidone (Esbriet) was purchased from Roche. The IC50 values of all three drugs were analyzed to determine the concentration to treat fibroblasts. Nintedanib and Pirfenidone were used at 1μM and 200μM respectively.

High-throughput screening

Primary murine adult cardiac fibroblasts were plated in 384 well (PerkinElmer ViewPlate-384 Black, Optically Clear Bottom, Tissue Culture Treated) using a Multidrop™ Combi Reagent Dispenser (Thermo Fisher Scientific), in order to obtain homogeneous seeding of the cells. The next day, an intermediate dilution (50μM; 0.5% DMSO in DMEM) of the FDA-approved compound library (640 compounds, ENZO Life Sciences) was prepared using the STARlet automated liquid handling station (Hamilton) and 10μl of this dilution was spotted on top of the cells, thus reaching a final concentration of 10μM with 0.1% DMSO. After additional 48 hours, the cells were fixed in 4% paraformaldehyde (PFA) for 10 minutes, washed in Phosphate Buffer Saline (PBS) and stained with both Hoechst 33342 (Thermo Fisher Scientific) and HCS Cell Mask Deep Red staining (Thermo Fisher Scientific). Image acquisition was performed using the ImageXpress Micro high content screening microscope (Molecular Devices) with a Nikon PlanFluor 10 x (NA=0.30) objective. A total of 4 fields per well were acquired and subsequently analysed for αSMA expression (TRITC channel, cellular mean fluorescence intensity) using the MetaXpress software (Molecular Devices) running the multi-wavelength cell scoring application module. The nuclear region was defined by an algorithm that segments the Hoechst 33342 channel signal using a combination of morphological parameters and pixel intensity over background. Cell viability was assessed by counting nuclei number. Upon assessment of normal distribution (Kolmogorov-Smirnov test), compounds exerting a toxic effect (z-score P≤0.10) were excluded from further

analysis. The average size of each cell was assessed by HCS Cell Mask Deep Red staining and the so defined region was interrogated for pixel intensity in the TRITC channel to estimate the average αSMA expression per cell.

Gene silencing

Silencing of Sigmar1 was performed in primary fibroblasts and NIH3T3, using the following shRNAs: TRCN0000193914 (shSigmar1_1), TRCN0000194512 (shSigmar1_2), TRCN0000292956 (shSigmar1_3), TRCN0000292958 (shSigmar1_4) obtained from Sigma Aldrich. Lentiviral particles expressing shRNAs were produced in 293T cells and used to transduce fibroblasts. Puromycin selection was initiated after 48 hours and continued for more than 3 days. Silencing of PERK was performed in primary fibroblasts with siPERK from SCBT (sc-36214) as per company instructions using transfection reagent Lipofectamine RNAiMax (Thermofischer). siUBC, obtained from Dharmacon, was used to determine transfection efficiency.

Immunoblotting and quantification

Protein lysates were prepared in lysis buffer containing 1% Triton X-100, 100mM Tris (pH 8.0), 100mM NaCl, 10mM EDTA, and run on Bis-Tris based polyacrylamide gels. Blocking of nitrocellulose membranes was done with 5% non-fat dry milk or 5% BSA. Densitometric analysis of bands was performed using ImageJ software. Integrated density of the area of the band and a similar size area from the background was measured. After background subtraction, normalization was done by dividing by the integrated density of the loading control followed by fold change compared to control condition.

Quantitative real time PCR

For quantitative real time PCR, RNA was extracted and purified by Trizol (Invitrogen) according to manufacturer's instructions, followed by cDNA synthesis using the M-MLV RT Kit from Invitrogen. Quantitative PCR was performed on a BioRad machine in a total volume of 10μl with 250nM primers and using *Gapdh* as a housekeeping gene. The sequences of the primers are provided in the Supplementary Table 5.

Calcium imaging

The fluorescent calcium indicator Fluo4/AM (Invitrogen) was used to estimate cytosolic calcium levels by either live imaging or using a plate reader. For live imaging, cells were washed with HBSS and loaded with 5μM Fluo4 in HBSS for 30 minutes at 37°C. Cells were imaged using a 40X oil-immersion objective at 100ms frame rate and a scanning confocal microscope (LSM 880 Carl Zeiss). The 488nm line of Argon laser was used to excite the fluorophore and images were collected at 520nm emission. Haloperidol was added during live imaging, approximately after 10 seconds (necessary to obtain a stable baseline). For microplate reader experiments, cells were plated in 96-wells plate and stained with Fluo4 as for confocal imaging. Subsequently they were placed in a multimode plate reader (Envision multilabel plate reader, PerkinElmer) equipped with

liquid handling for addition of appropriate drugs during the course of the experiments. Fluorescence was excited at 488nm and data collected at 520nm, every second. In both cases, data were analyzed using the F/F0 method, in which F represents the fluorescence at any time point, while F0 is the mean baseline fluorescence, averaged between either the first 10 frames for confocal imaging or the first 5 frames for multi-plate imaging.

Proliferation assays

Proliferation was assessed using 3-(4,5-dimethylthiazol-2-yl)-2,5-diphenyltetrazolium bromide (MTT) assay (Sigma-Aldrich) or crystal violet (Sigma-Aldrich) cell staining. Briefly, cells were washed once with PBS followed by incubation in media containing the MTT reagent for approximately 30 minutes. Cells with precipitated MTT were solubilized in 1% SDS and the optical signal read at 570 nm. For crystal violet staining, adherent cells were stained with 0.5% crystal violet solution in 25% methanol, washed and solubilized in 1% SDS. Optical absorbance was measured at 590 nm.

Migration assays

Migration was measured in a wound healing scratch assay. Fibroblasts were plated in 24 well plate with appropriate factors in 2% FBS DMEM media and let grow for 72 hours. After the monolayer formation, three scratches were made in the monolayer with p200 tip and the wound closure was monitored for 24 hours. Cells were fixed and stained with crystal violet and imaged for comparison of wound closure.

Luciferase reporter assays

The CAGA-Luc reporter was a gift from Dr. F. Loffredo, (ICGEB, Triese, Italy) and was used as previously reported (3). Firefly Luciferase Assay Kit (Biotium, Cat: 30075-1) was used for all assays. Briefly, 100,000 cells were plated in 24-well plates. The next day, cells were transfected with a CAGA-Luc reporter plasmid (2 μg) and GFP (1 μg) reporter plasmids using Lipofectamine 2000 (Invitrogen). The next day, the medium was changed with fresh medium containing TGFβ, Haloperidol and their combination. Cells were harvested after 48 hours in 100 μl of lysis buffer and luciferase activity determined by Envision plate reader (Perkin Elmer).

Collagen gel contraction assay

Collagen gel was prepared from homemade rat tail collagen. Prior to preparing collagen gel, fibroblasts were detached by trypsin/EDTA solution and resuspended in DMEM media. 300 μl of collagen gel with cells was prepared by mixing in the order of 50 μl of 8% $NaHCO_3$, 100 μl of 200,000 cell suspension, 150 μl of collagen solution and the contents were quickly transferred to 37° incubator for 1 hour for gel polymerization. Later 500 μl of media containing factors was added and gels were analyzed in the next days.

Docking studies

Haloperidol was structurally preprocessed using LigPrep from the Schrodinger Suite (4). Three different Haloperidol configurations were identified, considering pH values of 7.0 with a tolerance of +/- 2.0 unit of pH, as recommended by the Epik algorithm. Such penalty is considered in the final Docking Score, improving its ability of separating active compounds from inactive compounds. If this tolerance is omitted, i.e. if pH is set to 7.0 +/- 0.0, only the protonated state of Haloperidol is obtained. SiteMap binding site detector (5) was performed to detect druggable binding sites on both 5HK1 and 5HK2 structures. Five different binding sites for each trimer were detected. The developers of SiteMap suggest that a cut-off in the SiteScore of 0.80 can be used to differentiate between drug-binding and non-drug-binding sites, with scores higher than 1.0 being indicative of highly promising sites. Following these criteria, only the three high-ranked binding site for each trimer were considered (Supplementary Figure 7A). Molecular docking of Haloperidol ligand was conducted on each high-ranked druggable binding site of Sigmar1 receptor structures. The latter were preprocessed with the Protein Preparation Wizard from the Schrodinger Suite (4, 6-8). The protonation states of each side chain were generated using the software Epik (Schrödinger) for pH = 7 (6, 7). Protein energy minimization was performed using the OPLS3 force field (9, 10). Glide 75013 (11, 12) was used for all docking calculations. Internal and external receptor grid boxes of 10 × 10 × 10 and 20 × 20 × 20 Å were defined centered in the cupin-like β-barrel region. A standard precision (SP) Glide docking followed by Extra Precision (XP) refinement was carried out, generating at least two poses per docked molecule. Each docking result was analyzed by comparing the Glide Docking and eModel scores. The first is used for comparing different ligands, whereas the second score is suitable to rank different conformations of the same ligand.

Animal experiments

Myocardial infarction was performed as previously described (13). Briefly, 3 months old, male mice (either CD1 or COLL-EGFP) were anesthetized with ketamine/xylazine and connected to a mouse ventilator. The left anterior descending (LAD) coronary artery was ligated 1 mm below the left atrium auricula and the effective induction of cardiac ischemia was confirmed by the whitening of the heart anterior wall. Animals were kept on a heating pad at 37°C throughout the procedure. Mice were treated with Haloperidol at a concentration of 2mg/kg IP twice a week. Animals were sacrificed at either 10 days or 8 weeks.

For bleomycin induced fibrosis, a single bolus of bleomycin (0.03 U/mouse) was injected into the trachea of 3 months old, male COLL-EGFP mice. Haloperidol (2 mg/kg) was administered intraperitoneally twice a week and mice sacrificed at 10 days. For the comparative analysis of Haloperidol, Nintedanib and Pirfeindone in bleomycin induced fibrosis for preventive protocol; all three drugs were given orally once a day by gavage at the following concentrations: Haloperidol (2 mg/kg), Nintedanib (100 mg/kg) and Pirfenidone (100 mg/kg). Mice were sacrificed after 10 days.

For the comparative analysis of Haloperidol, Nintedanib and Pirfeindone in bleomycin induced fibrosis for therapeutic protocol, all three drugs were given orally once a day by gavage after 10 days of bleomycin at the following concentrations: Haloperidol (2 mg/kg), Nintedanib (100 mg/kg) and Pirfenidone (100 mg/kg). Mice were sacrificed after 10 days.

For the induction of lung cancer, lung adenocarcinoma LG1233 cells were injected into the tail vein of syngeneic, 3 months old, male C57BL/6 mice (100,000 cells per mouse). Haloperidol (2mg/kg) was administered intraperitoneally twice a week and mice were sacrificed at 10 days.

Echocardiography

To evaluate cardiac function, transthoracic two-dimensional echocardiography was performed on mice sedated with 5% isoflurane at 3, 5 and 8 weeks after myocardial infarction, using a Visual Sonics Vevo 2100 Ultrasound (FUJIFILM VisualSonics) equipped with a 30-MHz linear array transducer. The heart rate of all animals was kept over 400 beats per minute and the body temperature at 37°C. Systolic function was assessed on B-mode images, using a multi-planar evaluation (one long axis view and four short axis views at different levels of the left ventricle), for the quantitative estimation of systolic and diastolic volumes. The ejection fraction (EF) was calculated using a modified Simpson's rule, as per manufacturer's instructions (FUJIFILM VisualSonics). M-mode images were used to calculate fractional shortening (FS), end-diastolic left ventricular volume (EDLV) and end-systolic left ventricular volume (ESLV).

Histology

Immunocytochemistry was performed on 4% PFA fixed, 0.5% Triton X100-permeabilized and 5% BSA-blocked cells. Immunohistochemistry was performed either on PFA-fixed cryosections or PFA-fixed paraffin-embedded sections. Cryosections were air dried and dipped briefly in acetone followed by permeabilization in 0.5% Triton X100 for 20 minutes, blocking in 5% BSA for 1 hour, incubation with primary antibodies for 16 hours and with secondary antibodies for 1 hour. Paraffin-embedded sections were deparaffinized, hydrated and processed as described for cryosections. Sections of paraffin-embedded tumor-bearing lungs were stained with hematoxylin and eosin. Paraffin-embedded sections of the heart after myocardial infarction were processed for Masson Goldner trichrome staining (Carl Roth) to determine the fibrotic area, according to manufacturer's instructions. The infarct size was measured as the percentage of the total left ventricular area showing fibrosis. Following primary antibodies were used for immunofluorescence: αSMA – Cy3 (Sigma-Aldrich, clone 1A4), Vimentin (CST, D21H3), Ki-67 (CST, D3B5), Calreticulin (BD Biosciences, 612136).

Microscopy and image analysis

Microscopy was performed using a Leica microscope equipped with a DFC300 camera and Nikon Eclipse Ti-E inverted fluorescent microscope. Confocal microscopy was performed using Zeiss LSM 880 unit and Zeiss LSM 510 META microscopes. Images were analyzed using ImageJ (NIH).

Overlap of multiple color channels of confocal images was performed with JACoP plugin in ImageJ with default parameters.

Images were analyzed using the ImageJ NIH/Fiji software. RGB images were opened to manually select all cells having an intact nucleus using the 'ROI Manager'. Images were then split into 8-bit greyscale channels and the same ROI was copied to individual channels. Fluorescence intensity in each channel was then quantified by the function 'Analyze particles', upon background subtraction.

Tissue distribution of Haloperidol

Tissue samples weighing about 100 – 50mg were homogenized with MagNa Lyser instrument (Roche) in 250 μl of water before analysis by LC-MS-MS. The homogenate was then centrifuged and 125 μl of this homogenate was mixed with 200 μl of $NaHC0_3$, 350 μl of ethylacetate and 200 pg amount of internal standard (Haloperidol-D4, Cerilliant Corporation (Catalog number: H-002)). The mixture was vortexed and 150 μl of the organic phase was transferred to a new eppendorf. The extraction was performed twice and the organic layer was then evaporated in SpeedVac. Dried extracts were resuspended in 15 μl of 0.1% formic acid in water and 10 μl was injected onto a 170 mm x 0.150 mm custom packed column. The column was custom packed using 5 μm Ascentis Express RPA resin (Sigma Aldrich). The column was developed over 15 mins using a 0.1% formic acid in water to 80% acetonitrile gradient. The effluent of the column was sprayed directly into an Amazon ETD mass spectrometer (Bruker Daltonics). Haloperidol was selectively fragmented which produced two diagnostic ions at 167 and 123 m/z, and the deuterium labeled Haloperidol producing ions at 169 and 127 m/z. Haloperidol was fragmented using a trap amplitude of 0.5 for 40 ms. The fragments at 167 and 169 were used to quantitate the levels of Haloperidol. Calibration curves using lung tissue were set up using a 200 pg of deuterated Haloperidol and a range of 20 to 500 pg of unlabeled Haloperidol.

Supplementary references

1. Magness, S.T., Bataller, R., Yang, L., and Brenner, D.A. 2004. A dual reporter gene transgenic mouse demonstrates heterogeneity in hepatic fibrogenic cell populations. *Hepatology* 40:1151-1159.
2. Dimitrova, N., Gocheva, V., Bhutkar, A., Resnick, R., Jong, R.M., Miller, K.M., Bendor, J., and Jacks, T. 2016. Stromal Expression of miR-143/145 Promotes Neoangiogenesis in Lung Cancer Development. *Cancer Discov* 6:188-201.
3. Dennler, S., Itoh, S., Vivien, D., ten Dijke, P., Huet, S., and Gauthier, J.M. 1998. Direct binding of Smad3 and Smad4 to critical TGF beta-inducible elements in the promoter of human plasminogen activator inhibitor-type 1 gene. *EMBO J* 17:3091-3100.
4. Sastry, G.M., Adzhigirey, M., Day, T., Annabhimoju, R., and Sherman, W. 2013. Protein and ligand preparation: parameters, protocols, and influence on virtual screening enrichments. *Journal of Computer-Aided Molecular Design* 27:221-234.
5. Halgren, T.A. 2009. Identifying and characterizing binding sites and assessing druggability. *Journal of Chemical Information and Modeling* 49:377-389.
6. Greenwood, J.R., Calkins, D., Sullivan, A.P., and Shelley, J.C. 2010. Towards the comprehensive, rapid, and accurate prediction of the favorable tautomeric states of drug-like molecules in aqueous solution. *Journal of Computer-Aided Molecular Design* 24:591-604.
7. Shelley, J.C., Cholleti, A., Frye, L.L., Greenwood, J.R., Timlin, M.R., and Uchimaya, M. 2007. Epik: a software program for pK a prediction and protonation state generation for drug-like molecules. *Journal of Computer-Aided Molecular Design* 21:681-691.
8. Jacobson, M.P., Friesner, R.A., Xiang, Z., and Honig, B. 2002. On the Role of the Crystal Environment in Determining Protein Side-chain Conformations. *Allosteric Interactions and Biological Regulation (Part II)* 320:597-608.
9. Harder, E., Damm, W., Maple, J., Wu, C., Reboul, M., Xiang, J.Y., Wang, L., Lupyan, D., Dahlgren, M.K., Knight, J.L., et al. 2016. OPLS3: A Force Field Providing Broad Coverage of Drug-like Small Molecules and Proteins. *Journal of Chemical Theory and Computation* 12:281-296.
10. Jorgensen, W.L., Maxwell, D.S., and Tirado-Rives, J. 1996. Development and Testing of the OPLS All-Atom Force Field on Conformational Energetics and Properties of Organic Liquids. *Journal of the American Chemical Society* 118:11225-11236.
11. Friesner, R.A., Banks, J.L., Murphy, R.B., Halgren, T.A., Klicic, J.J., Mainz, D.T., Repasky, M.P., Knoll, E.H., Shelley, M., Perry, J.K., et al. 2004. Glide: a new approach for rapid, accurate docking and scoring. 1. Method and assessment of docking accuracy. *Journal of Medicinal Chemistry* 47:1739-1749.
12. Halgren, T.A., Murphy, R.B., Friesner, R.A., Beard, H.S., Frye, L.L., Pollard, W.T., and Banks, J.L. 2004. Glide: a new approach for rapid, accurate docking and scoring. 2. Enrichment factors in database screening. *Journal of Medicinal Chemistry* 47:1750-1759.
13. Eulalio, A., Mano, M., Dal Ferro, M., Zentilin, L., Sinagra, G., Zacchigna, S., and Giacca, M. 2012. Functional screening identifies miRNAs inducing cardiac regeneration. *Nature* 492:376-381.

Supplementary figure 1

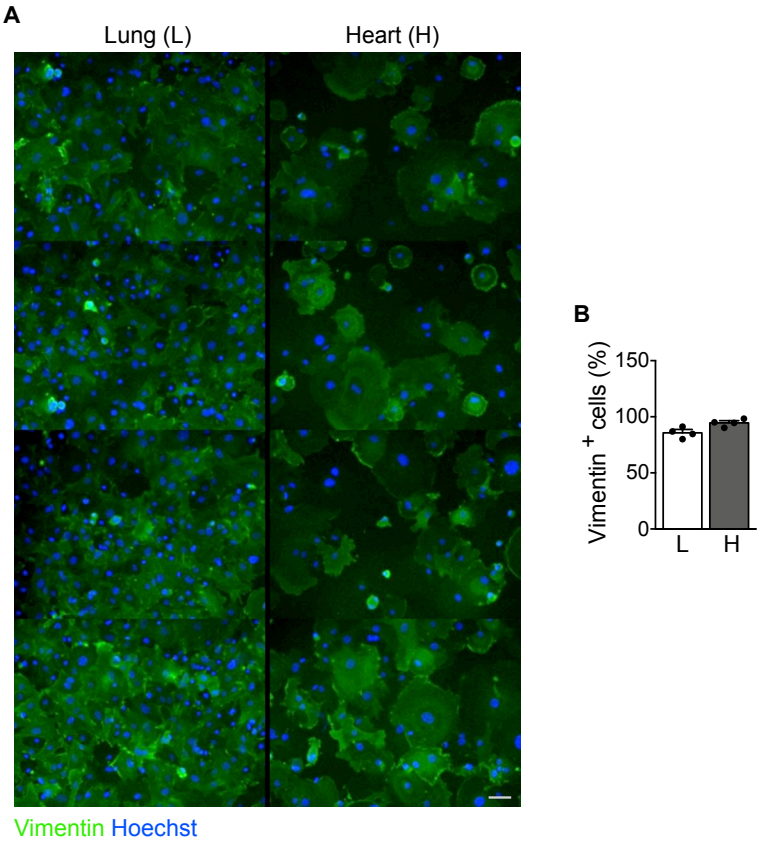

Supplementary Figure 1. Purity of fibroblast isolation. (**A**) Primary fibroblasts from lung (L) and heart (H) stained with anti-vimentin antibodies (green). Nuclei are stained in blue with Hoechst. Scale bar, 15μm. (**B**) Quantification of the percentage of vimentin$^+$ cells in primary cultures of fibroblasts from lung (L) and heart (H) (n = 4/gp). Values are mean ± SEM.

Supplementary figure 2.

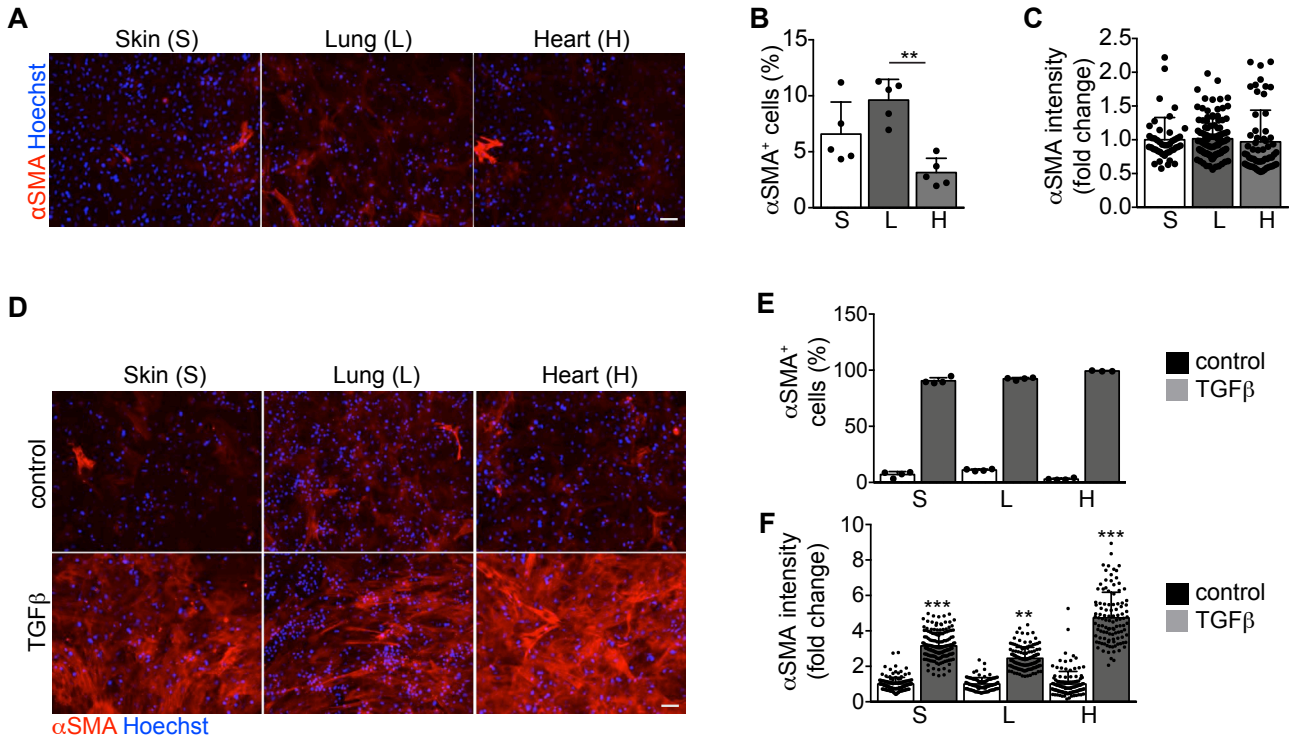

Supplementary Figure 2. Fibroblasts from different tissues are differentially prone to undergo myofibroblast differentiation. (**A**) Primary fibroblasts from skin (S), lung (L) and heart (H) are stained with anti-αSMA antibodies (red) and nuclei are stained blue with Hoechst. (**B**) Quantification of the number of αSMA$^+$ fibroblasts from skin (S), lung (L) and heart (H) (n = 5/gp). (**C**) Quantification of the αSMA mean fluorescence intensity in fibroblasts from skin (S), lung (L) and heart (H) (n > 44 cells/gp). (**D**) Primary fibroblasts from skin (S), lung (L) and heart (H) are stained with anti-αSMA antibodies (red) upon treatment with TGFβ (25 ng/ml) for 72 hours. Nuclei are stained in blue with Hoechst. (**E**) Quantification of the number of αSMA$^+$ positive fibroblasts from skin (S), lung (L) and heart (H) upon TGFβ stimulation (n = 4/gp). (**F**) Quantification of the αSMA mean fluorescence intensity in fibroblasts from skin (S), lung (L) and heart (H) upon TGFβ stimulation (n > 40/gp) Values in B and E are mean ± SEM. Values in C and F are mean ± SD, representative of three independent experiments with similar results.*P<0.05, **P<0.01, ***P<0.001 by unpaired t-test. Scale bar in A and D, 50μm.

Supplementary figure 3.

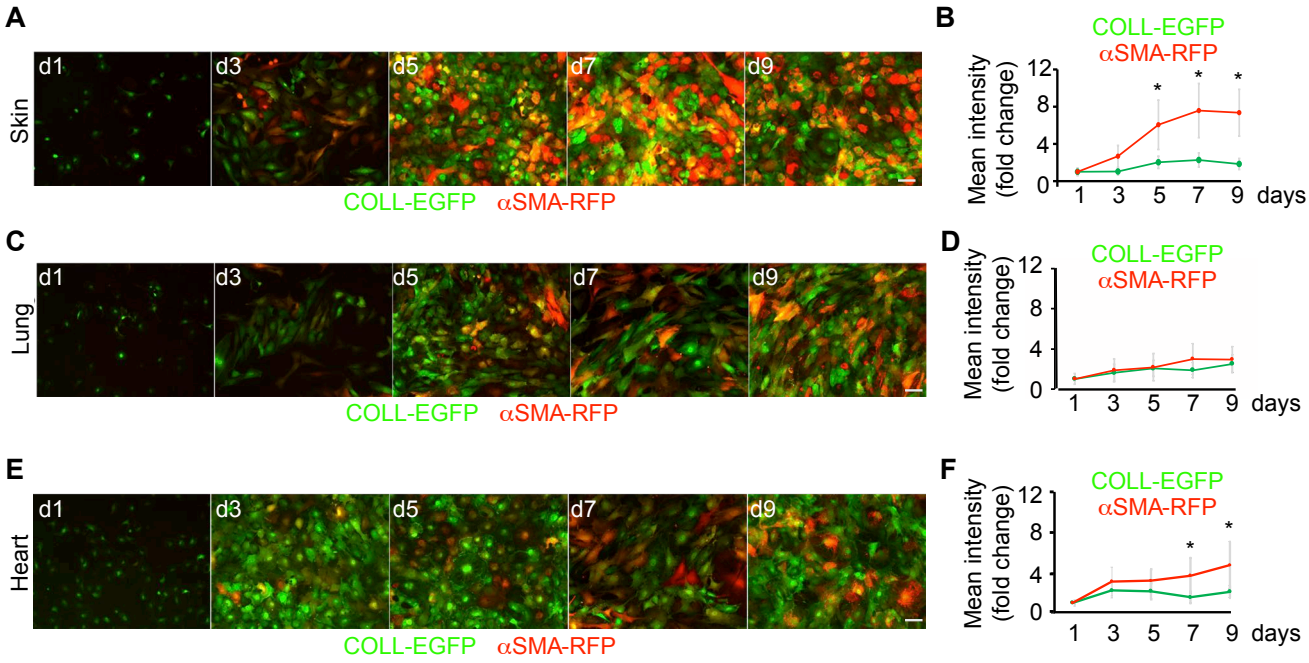

Supplementary Figure 3. **Primary fibroblasts from skin, lung and heart of αSMA-RFP/COLL-EGFP mice undergo spontaneously differentiation over time. Green fluorescence indicates collagen expression, whereas red fluorescence indicates αSMA expression.** (**A**) Representative images of skin fibroblasts from day 1 (d1) to day 9 (d9) of culture. (**B**) Quantification of the αSMA (red line) and collagen (green line) mean fluorescence intensity in skin fibroblasts from αSMA-RFP/COLL-EGFP mice over time. (**C**) Representative images of lung fibroblasts from day 1 (d1) to day 9 (d9) of culture. (**D**) Quantification of the αSMA (red line) and collagen (green line) mean fluorescence intensity in lung fibroblasts from αSMA-RFP/COLL-EGFP mice over time. (**E**) Representative images of heart fibroblasts from day 1 (d1) to day 9 (d9) of culture. (**F**) Quantification of the αSMA (red line) and collagen (green line) mean fluorescence intensity in heart fibroblasts from αSMA-RFP/COLL-EGFP mice over time. Values are mean ± SEM relative to day 1. *P<0.05 by unpaired t-test. Scale bar in A, C, E, 50μm.

Supplementary figure 4.

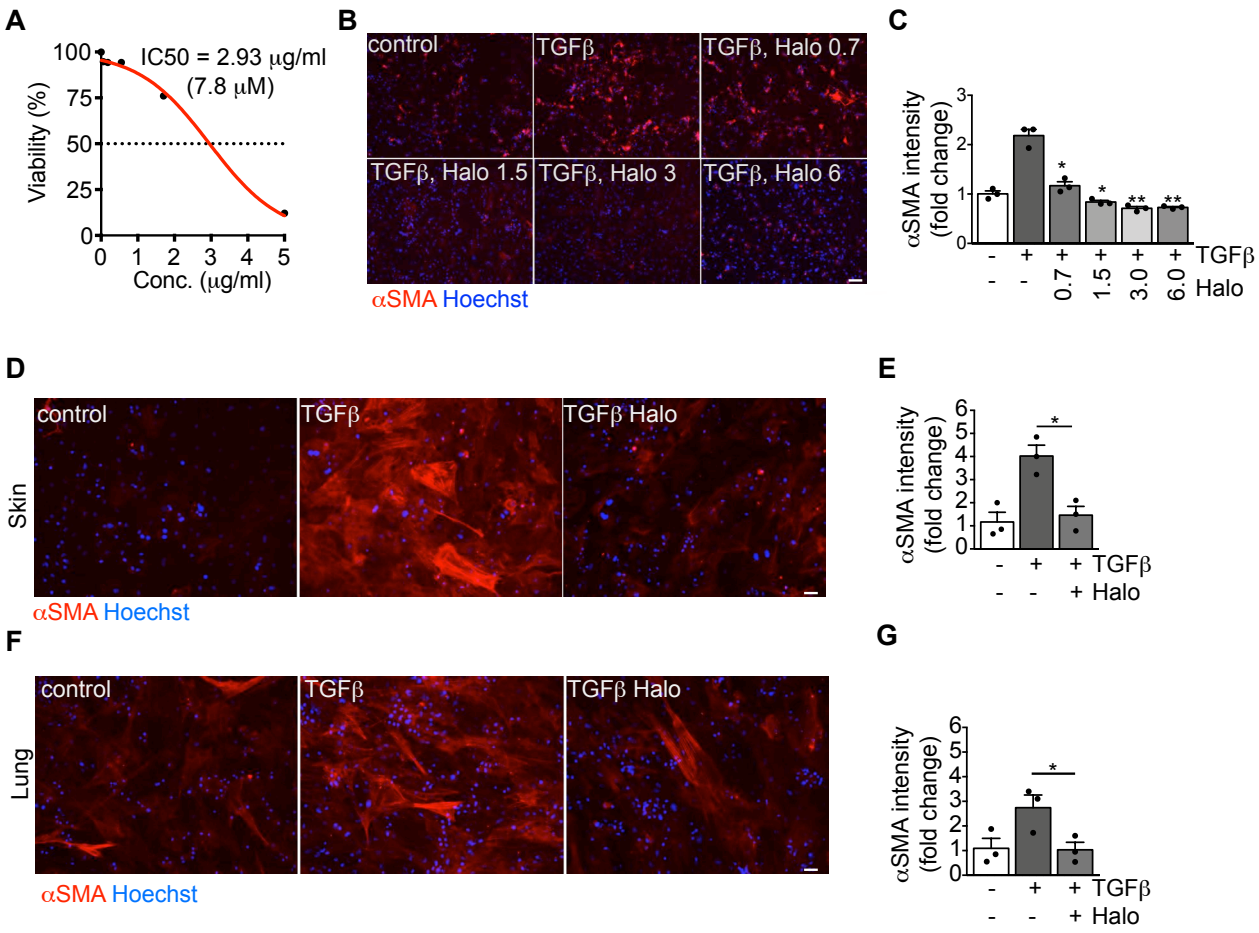

Supplementary Figure 4. Fibroblasts from different tissues comparably respond to haloperidol. (**A**) Different concentrations (conc.) of Haloperidol were tested on cardiac fibroblasts and viability assessed by MTT assay. Every dot shows the mean of a biological duplicate. The dose of Haloperidol killing 50% of the cells is indicated as IC50. (**B**) Representative images of αSMA-stained cardiac fibroblasts (red) treated with TGFβ, Haloperidol and their combination with increasing concentrations of Haloperidol (0.7, 1.5, 3 and 6 µM). Nuclei are stained in blue with Hoechst. (**C**) Quantification of the αSMA mean fluorescence intensity upon treatment with TGFβ, Haloperidol and their combination with the indicated dose (µM) of Haloperidol (n =3/gp). (**D**) Primary skin fibroblasts treated with TGFβ, Haloperidol and their combination and stained with anti-αSMA antibodies. Nuclei are stained in blue with Hoechst. (**E**) Quantification of the αSMA mean fluorescence intensity in skin fibroblasts upon treatment with TGFβ, Haloperidol and their combination with Haloperidol (n =3/gp). (**F**) Primary lung fibroblasts treated with TGFβ, Haloperidol and their combination and stained with anti-αSMA antibodies. Nuclei are stained in blue with Hoechst. (**G**) Quantification of the αSMA mean fluorescence intensity in lung fibroblasts upon treatment with TGFβ, Haloperidol and their combination (n =3/gp). Scale bar in B, D and F, 50µm. Values in C, E and G are mean ± SEM Significance in the C are shown compared to TGFβ). *P<0.05, **P<0.01, ***P<0.001 by unpaired t-test. (

Supplementary figure 5.

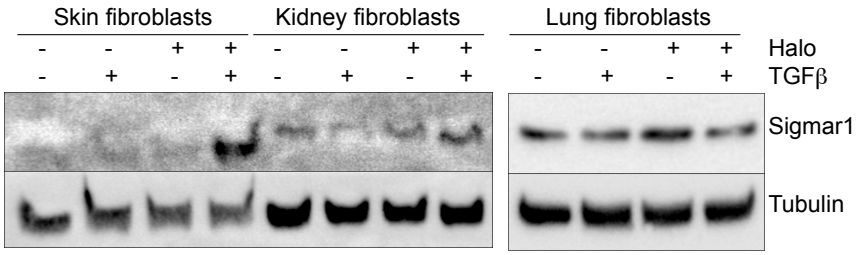

Supplementary Figure 5. Haloperidol up-regulates Sigmar1 in fibroblasts. Western blot showing the expression of Sigmar1 upon treatment with TGFβ, Haloperidol and their combination in primary adult skin, kidney, and lung fibroblasts. Tubulin is used as a loading control.

Supplementary figure 6.

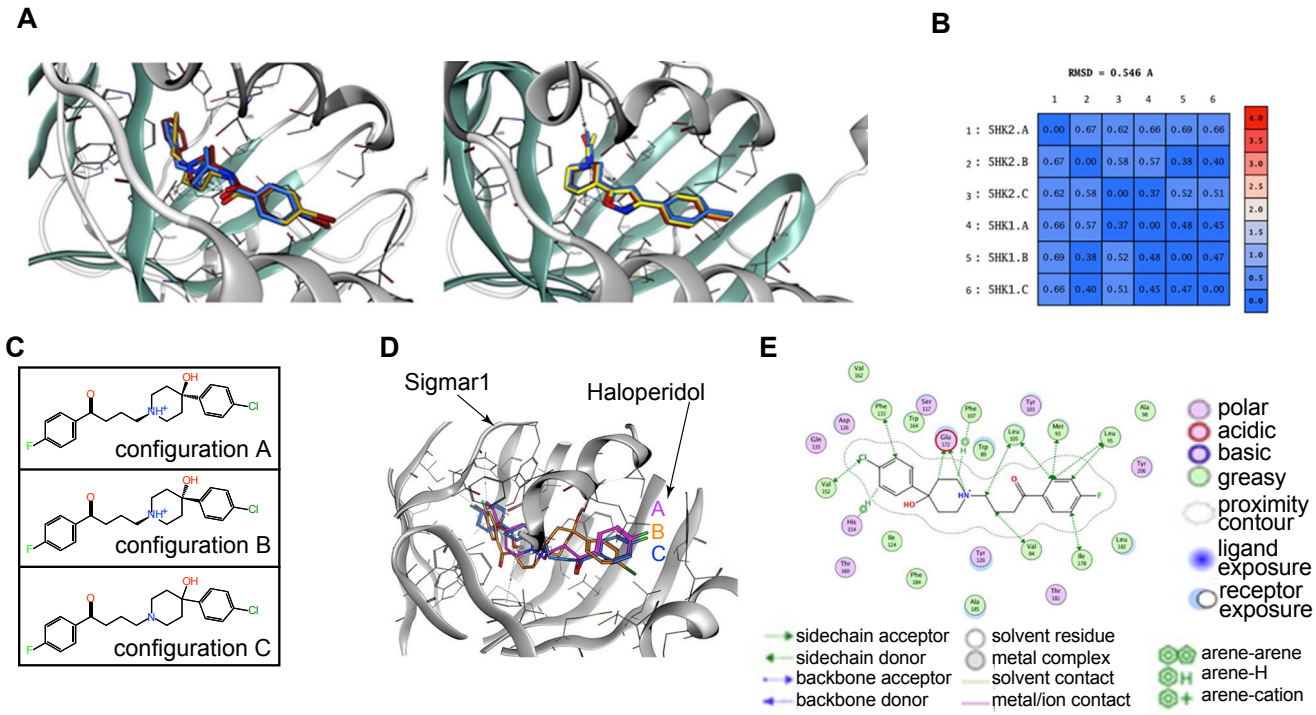

Supplementary Figure 6. Molecular docking of Haloperidol in Sigmar1. (**A**) Superimposition of the three Sigmar1 binding sites in 5HK1 (left) and 5HK2 (right) monomers with the known ligands, 3-(4-methylphenyl)-5-(1-propyl-3,6-dihydro-2H-pyridin-5-yl)-1,2-oxazole and N-(1-benzylpiperidin-4-yl)-4-iodobenzamide. Red, blue and yellow corresponds to the three main configurations of the ligands bound to each Sigmar1 monomer. The Sigmar1 protein is in cartoon representation. (**B**) Root Main Square Deviation (RMSD) in Armstrong (Å) of the six identified binding sites. (**C**) Two-dimensional structure of the three different Haloperidol configurations at pH=7 evaluated with LigPrep, Schrodinger Suite. Atom color assignment: black, carbon; red, oxygen; green, halogen; blue, nitrogen. (**D**) Tri-dimensional view of the highest ranked binding poses for the three configurations of Haloperidol shown in c. Sigmar1 protein is represented in grey cartoon, while the ligands are in purple (configuration A), orange (configuration B) and blue (configuration C). (**E**) Schematic representation of the highest ranked Haloperidol binding pose (5HK1 chain B Halo conf. A) according to Glide Docking and Emodel score, with indication of the nature of residues interacting with Haloperidol within the binding cavity of Sigmar1.

Supplementary figure 7.

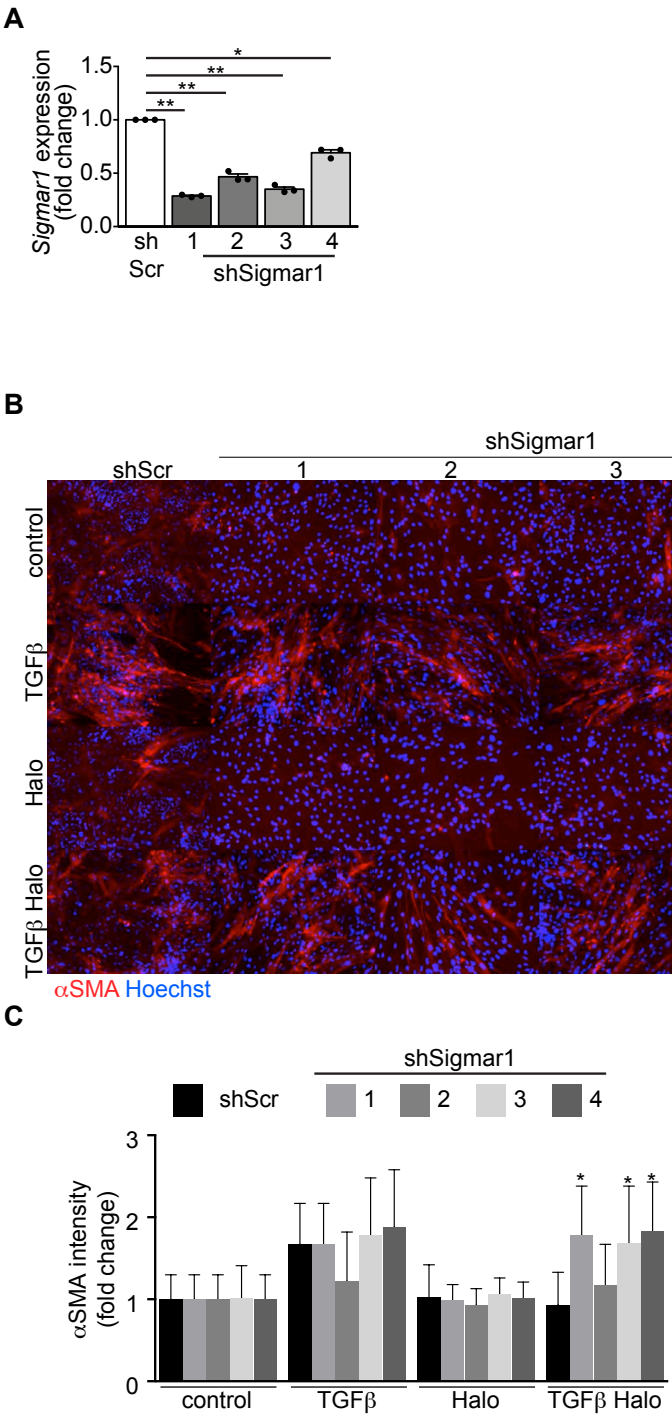

Supplementary Figure 7. Haloperidol requires Sigmar1 to inhibit αSMA expression in NIH3T3 cells. (**A**) Quantitative real time PCR for mRNA expression of *Sigmar1* after its silencing with four different shRNAs in NIH3T3 cells (n = 3/gp). The scrambled sequence of shSigmar1-1 was used a control. (**B**) αSMA staining (red) of NIH3T3 cells after Sigmar1 silencing with the four shRNAs and treatment with TGFβ, Haloperidol and their combination. Nuclei are stained in blue with Hoechst. Scale bar, 50 μm. (**C**) Quantification of the mean αSMA intensity in NIH3T3 cells after Sigmar1 silencing with the four shRNAs and treatment with TGFβ, Haloperidol and their combination (n = 3/gp). Values in A and C are mean ± SEM. *P<0.05, **P<0.01 relative to control by unpaired t-test.

Supplementary figure 8.

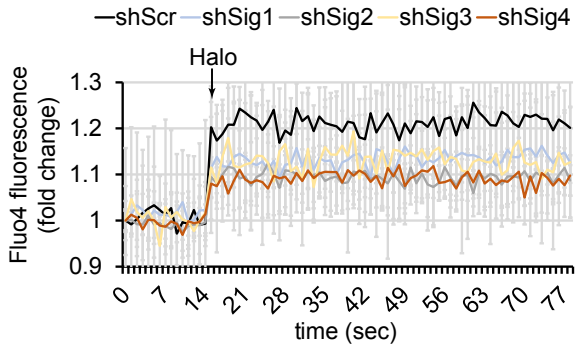

Supplementary Figure 8. **Effect of Sigmar1 silencing on Haloperidol-induced Fluo4 fluorescence activity.** Quantification of the Fluo4 fluorescence intensity in NIH3T3 cells treated with Haloperidol (arrow) in combination with either a scrambled shRNA (black line) or the four shRNAs silencing Sigmar1 (blue, grey, yellow and orange lines). The average of three biological replicates with SD is plotted.

Supplementary figure 9.

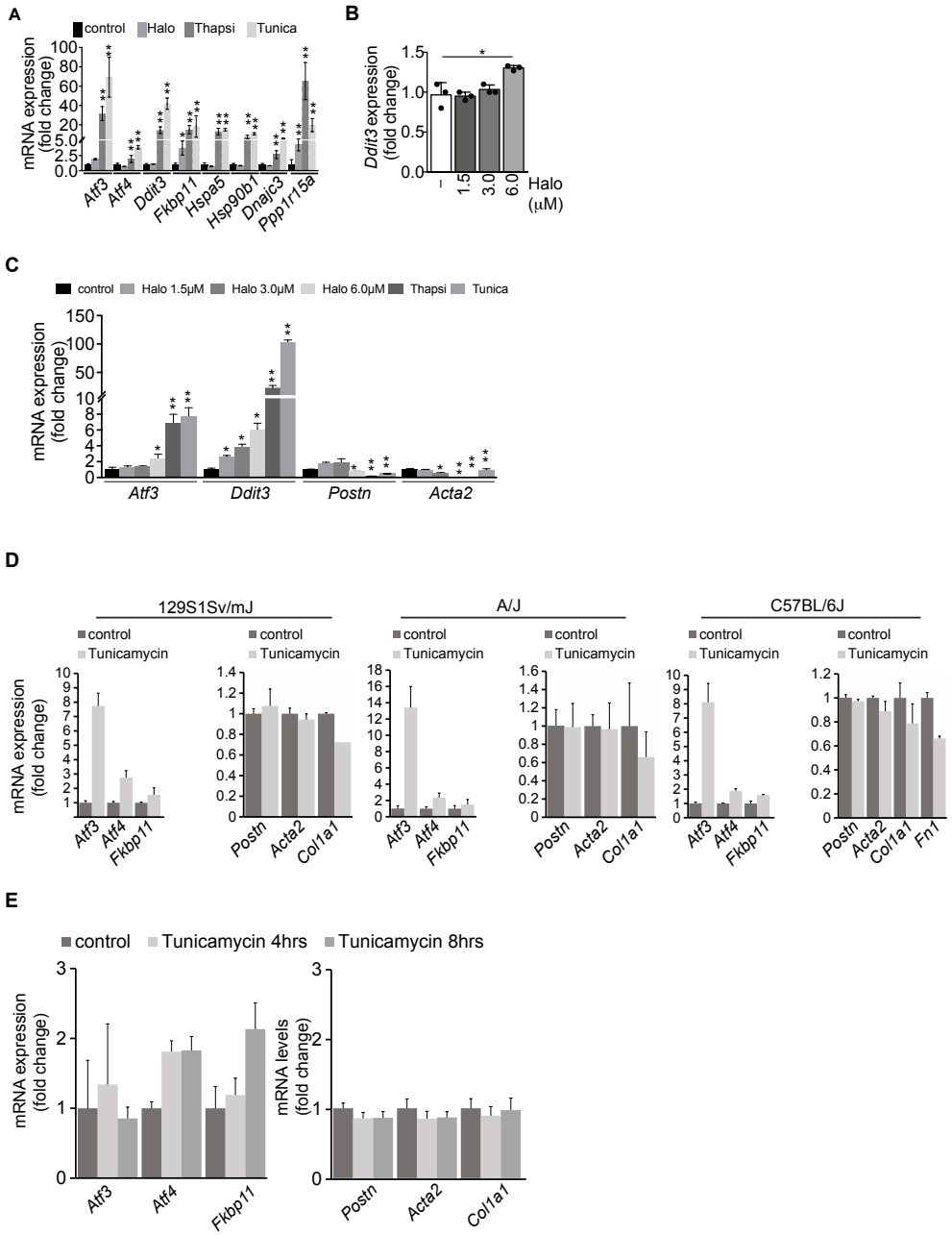

Supplementary Figure 9. Analysis of ER stress and fibrotic genes in different fibroblasts. (**A**) Levels of mRNA expression of activating transcription factor 3 and 4 (*Atf3, Atf4)*, DNA-damage inducible transcript 3 (*Ddit3*), FK506 binding protein 11 (*Fkbp11)*, heat shock protein 5 *(Hspa5)*, heat shock protein 90, beta member 1 *(Hsp90b1/Grp94)*, DnaJ Hsp40 member C3 (*Dnajc3)* and protein phosphatase 1, regulatory subunit 15A *(Ppp1r15a / Gadd34),* upon treatment with Haloperidol, Thapsigargin, and Tunicamycin (n = 3/gp). (**B**) Levels of *Ddit3* in response to the indicated doses of Haloperidol (n = 3/gp). (**C**) Real-time quantification of mRNA expression of *Atf3*, *Chop*, *Postn* and *Acta2* in primary adult murine lung fibroblasts treated with increasing doses of Haloperidol (Halo), Thapsigargin (Thapsi) and Tunicamycin (Tunica) (n = 3/gp). (**D**) Analysis of mRNA expression of the indicated genes upon treatment of mouse embryonic fibroblasts (MEFs) from the indicated strains with Tunicamycin, as reported in the publicly available microarray dataset GSE63756. (**E**) Analysis of mRNA expression of the indicated genes upon treatment of C57BL/6 mouse embryonic fibroblasts (MEFs) with Tunicamycin at the indicated time points, as reported in the publicly available microarray dataset GSE2082. Values in A, B, C, D and E are mean ± SEM. *P<0.05, **P<0.01 by unpaired t-test relative to control.

Supplementary figure 10.

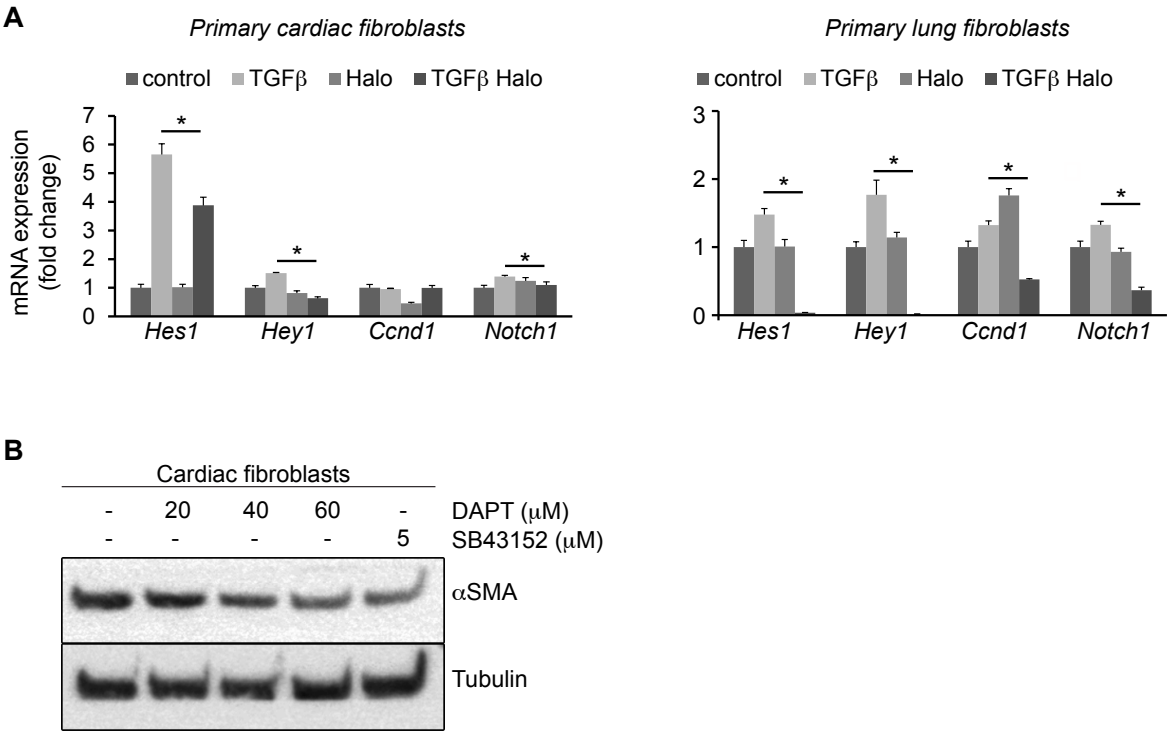

Supplementary Figure 10. Regulation of the Notch pathway by Haloperidol. (**A**) Quantification of the mRNA expression of the Notch target genes *Hes1*, *Hey1*, *Ccnd1* and *Notch1* itself, after 3 days of treatment with TGFβ alone or in combination with Haloperidol in cardiac and lung fibroblasts. (n = 3/gp). Values are mean ± SEM. *P<0.05 by unpaired two tailed t-test with Welch's correction relative to control (**B**) Western blot showing the expression of αSMA levels upon treatment of cardiac fibroblasts with the indicated doses of either the gamma secretase inhibitor DAPT or the TGFβ inhibitor SB43152. Tubulin is used as a loading control.

Supplementary figure 11.

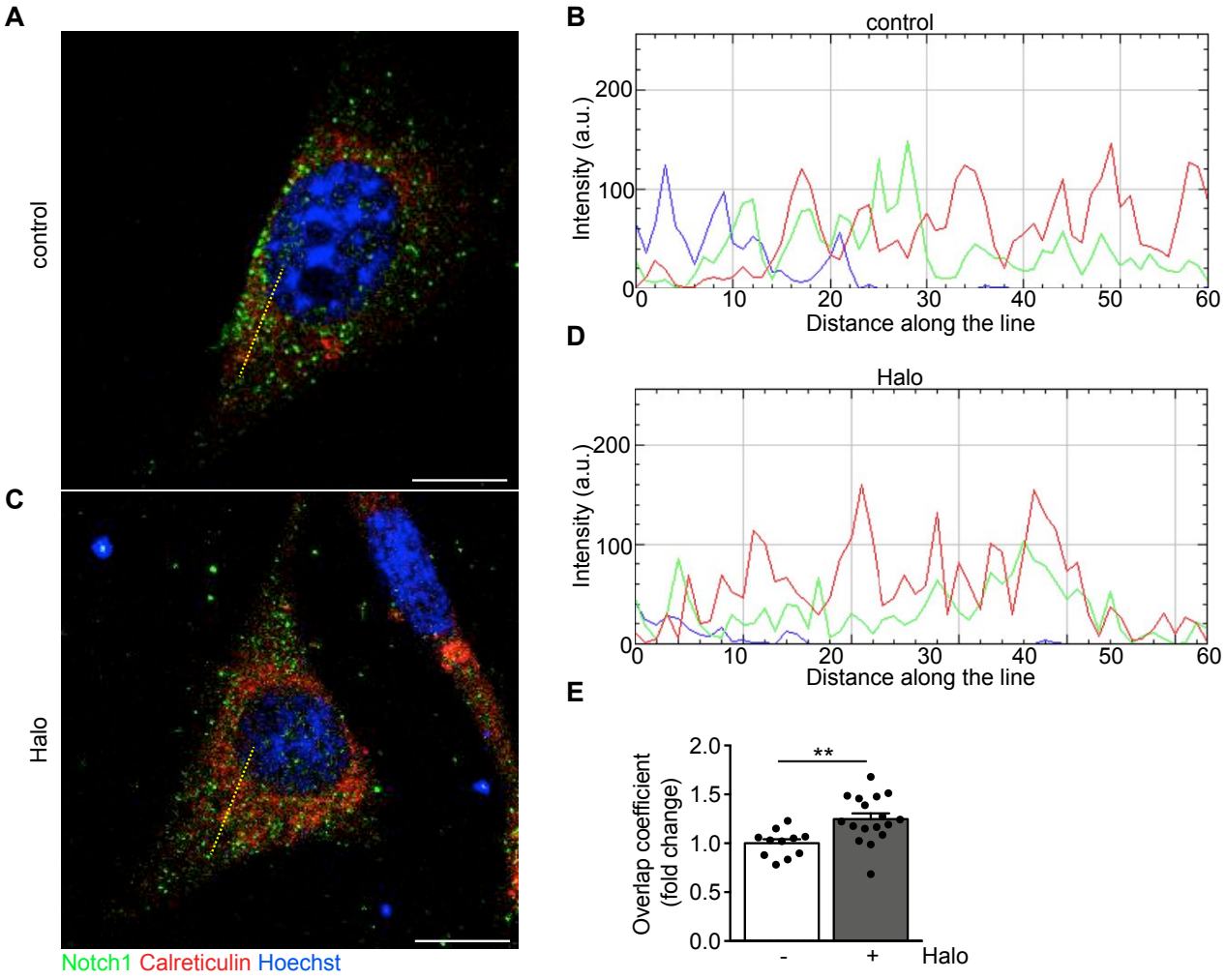

Supplementary Figure 11. **Localization of Notch1 with ER marker upon Haloperidol treatment and effect on Golgi complex.** (**A,C**) Representative images of untreated cardiac fibroblasts or treated with Haloperidol for 72 hours and stained with anti-Notch1 (green) and anti-Calreticulin (red) antibodies. Nuclei are stained in blue with Hoechst. (**B,D**) RGB profile on the dashed line marked in (A,C). (**E**) Quantification of overlap coefficient between Notch1 and Calreticulin in untreated fibroblasts and treated with Haloperidol (n >11/gp). Values are mean ± SD. Data are representative of three independent experiments with similar results. **P<0.01 by unpaired t-test relative to control. Scale bar in A,C, 10μm.

Supplementary figure 12.

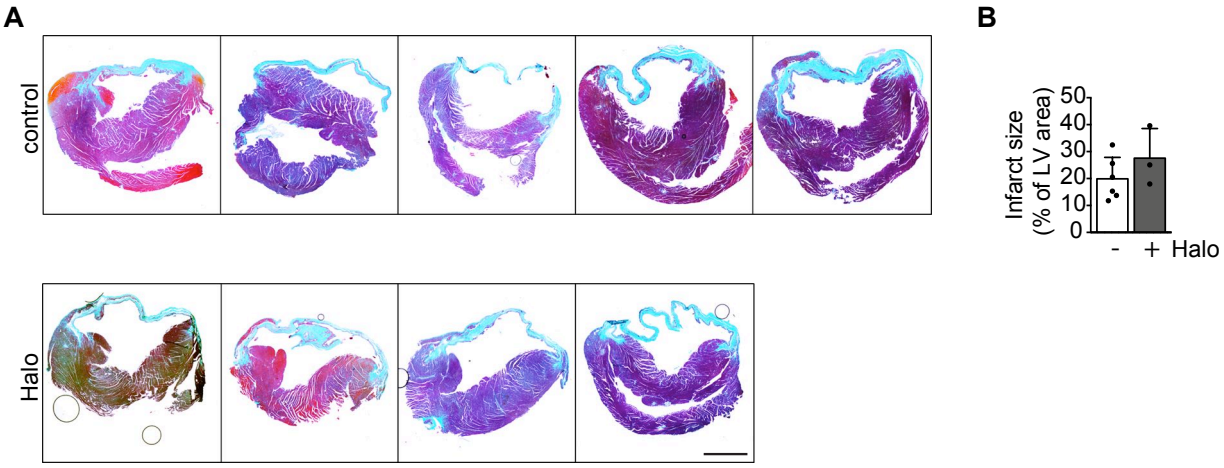

Supplementary Figure 12. Outcome of MI. (**A**) Masson Trichrome staining of heart sections of mice treated with either PBS (control) or Haloperidol treated at 8 weeks after MI. (**B**) Quantification of infarct size in the hearts of mice treated with either PBS (control) or Haloperidol treated at 8 weeks after MI (n >5/gp). Values are mean ± SEM. Scale bar, 1 mm.

Supplementary Figure 13.

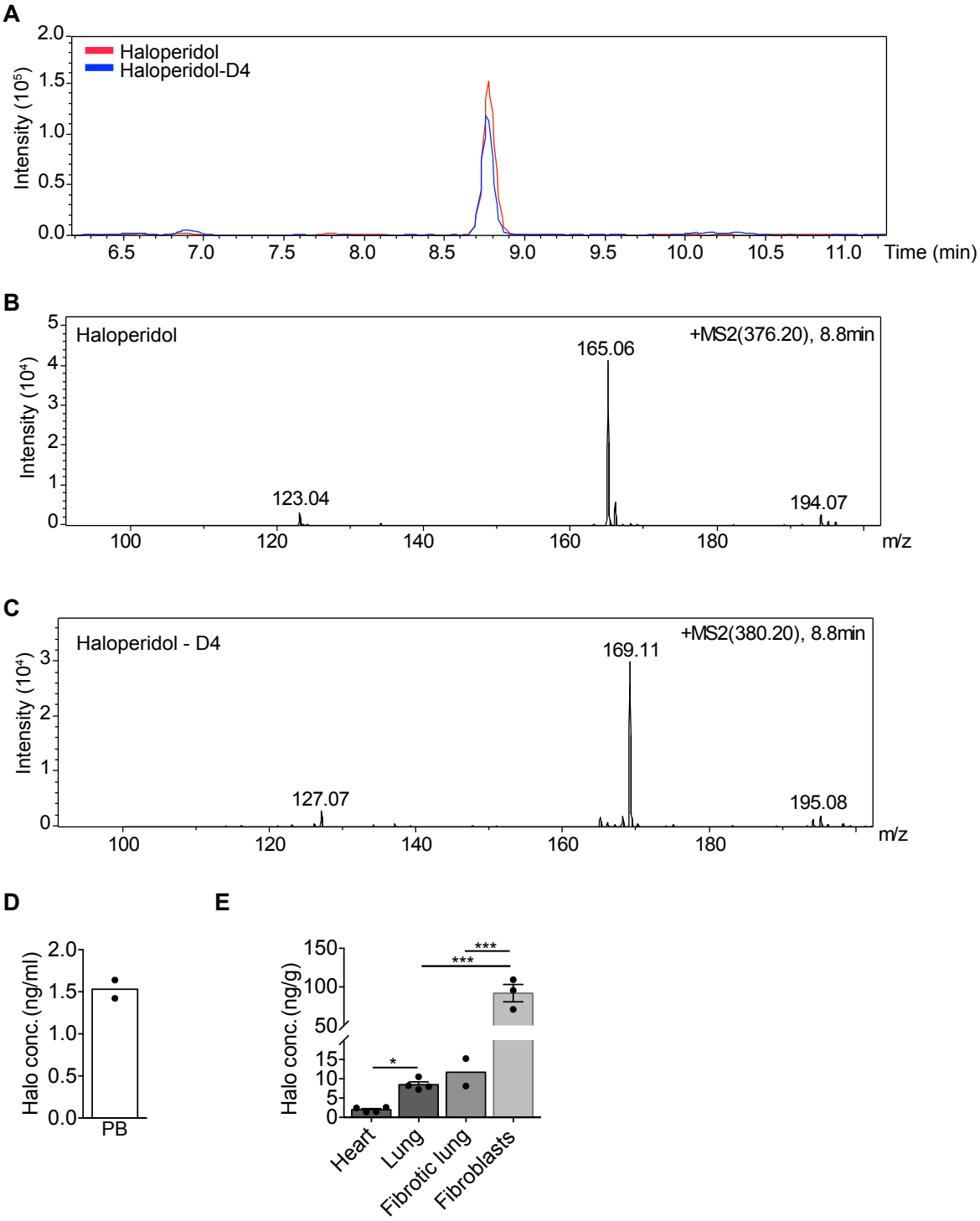

Supplementary Figure 13. Tissue distribution of Haloperidol. (**A**) Representative chromatogram of a mixture of Haloperidol and Haloperidol-D4. (**B**) MS/MS spectra of Haloperidol. (**C**) MS/MS spectra of Haloperidol-D4. (**D**) Tissue concentration of Haloperidol in peripheral blood (PB) (n = 2). (**E**) Tissue concentration of Haloperidol in heart (n = 4), lung (n = 4), bleomycin-treated, fibrotic lungs (n = 2) and primary lung fibroblasts in culture (n = 3). Values are mean ± SEM. *P<0.05, ***P<0.001 by unpaired t-test.

Supplementary figure 14.

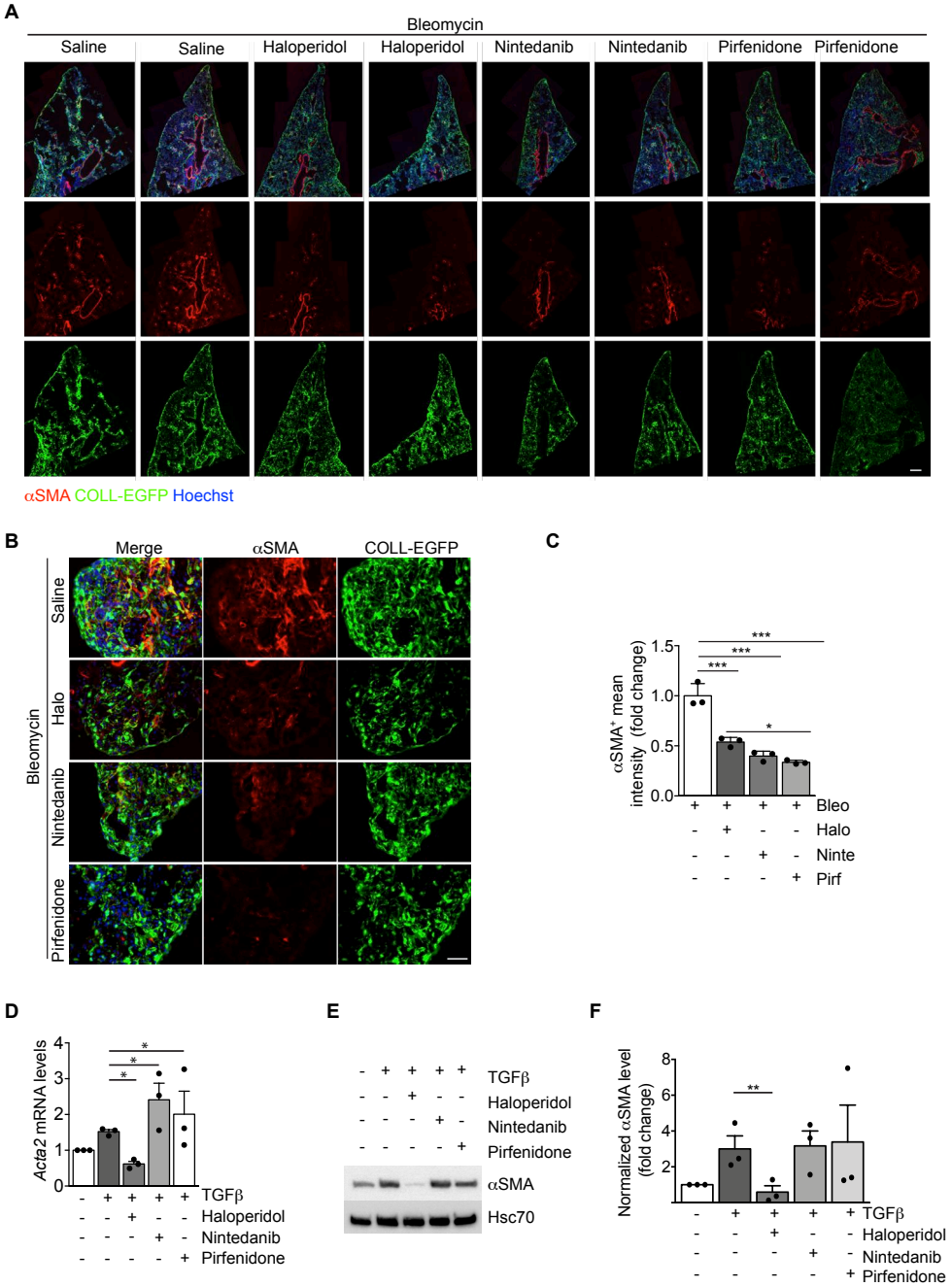

Supplementary Figure 14. Comparison of the effect of Haloperidol, Nintedanib and Pirfenidone in a preventive protocol. (**A**) Representative images of lung sections of COLL-EGFP mice exposed to Bleomycin and treated with Haloperidol, Nintedanib and Pirfenidone and stained with anti-αSMA antibody (white). Nuclei are stained in blue with Hoechst. (**B**) Higher magnification images of extravascular regions of lungs of COLL-EGFP mice exposed to Bleomycin and treated with Haloperidol, Nintedanib and Pirfenidone. (**C**) Quantification of the αSMA mean intensity in fibroblasts of lungs exposed to Bleomycin and treated with Haloperidol, Nintedanib and Pirfenidone (n = 3/gp). (**D**) Real-time quantify cation of mRNA expression of *Acta2* normalized to *Gapdh* in primary adult murine lung fibroblasts treated with TGFβ alone and in combination with Haloperidol, Nintedanib and Pirfenidone (n = 3/gp). (**E**) Western blot showing the expression of αSMA upon treatment of lung fibroblasts with TGFβ alone and in combination with Haloperidol, Nintedanib and Pirfenidone. Hsc70 is used as loading control. (**F**) Densitometric analysis of αSMA normalized to Hsc70 (n = 3/gp). Scale bar, 1 mm in A; 25μm in B. Values in C, D and F are mean ± SEM. *P<0.05, **P<0.01, ***P<0.001 by one-way ANOVA and Dunnett's multiple comparisons post-hoc test in C and unpaired t-test in D and F.

Supplementary figure 15.

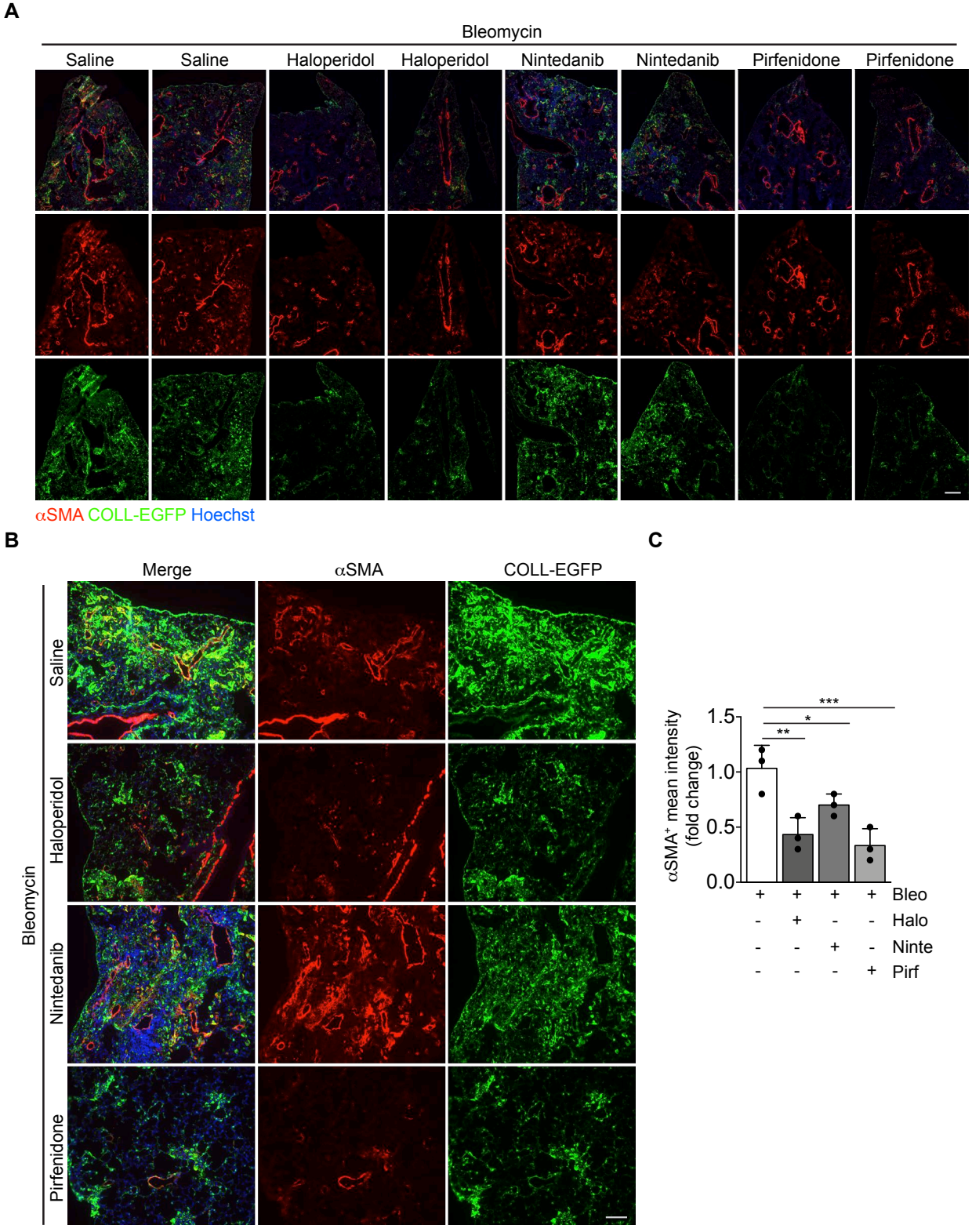

Supplementary Figure 15. **Comparative analysis of Haloperidol, Nintedanib and Pirfenidone in a therapeutic protocol.** (**A**) Representative images of lung sections of COLL-EGFP mice exposed to Bleomycin and treated with Haloperidol, Nintedanib and Pirfenidone and stained with anti-αSMA antibody (white). Nuclei are stained in blue with Hoechst. (**B**) Higher magnification images of extravascular regions of lungs of COLL-EGFP mice exposed to Bleomycin and treated with Haloperidol, Nintedanib and Pirfenidone. (**C**) Quantification of the αSMA mean intensity in fibroblasts of lungs exposed to Bleomycin and treated with Haloperidol, Nintedanib and Pirfenidone (n = 3/gp). Values are mean ± SEM. *P<0.05, **P<0.01, ***P<0.001 001 by one-way ANOVA and Dunnett's multiple comparisons post-hoc test. Scale bar, 1 mm in A; 25 μm in B.

Supplementary figure 16.

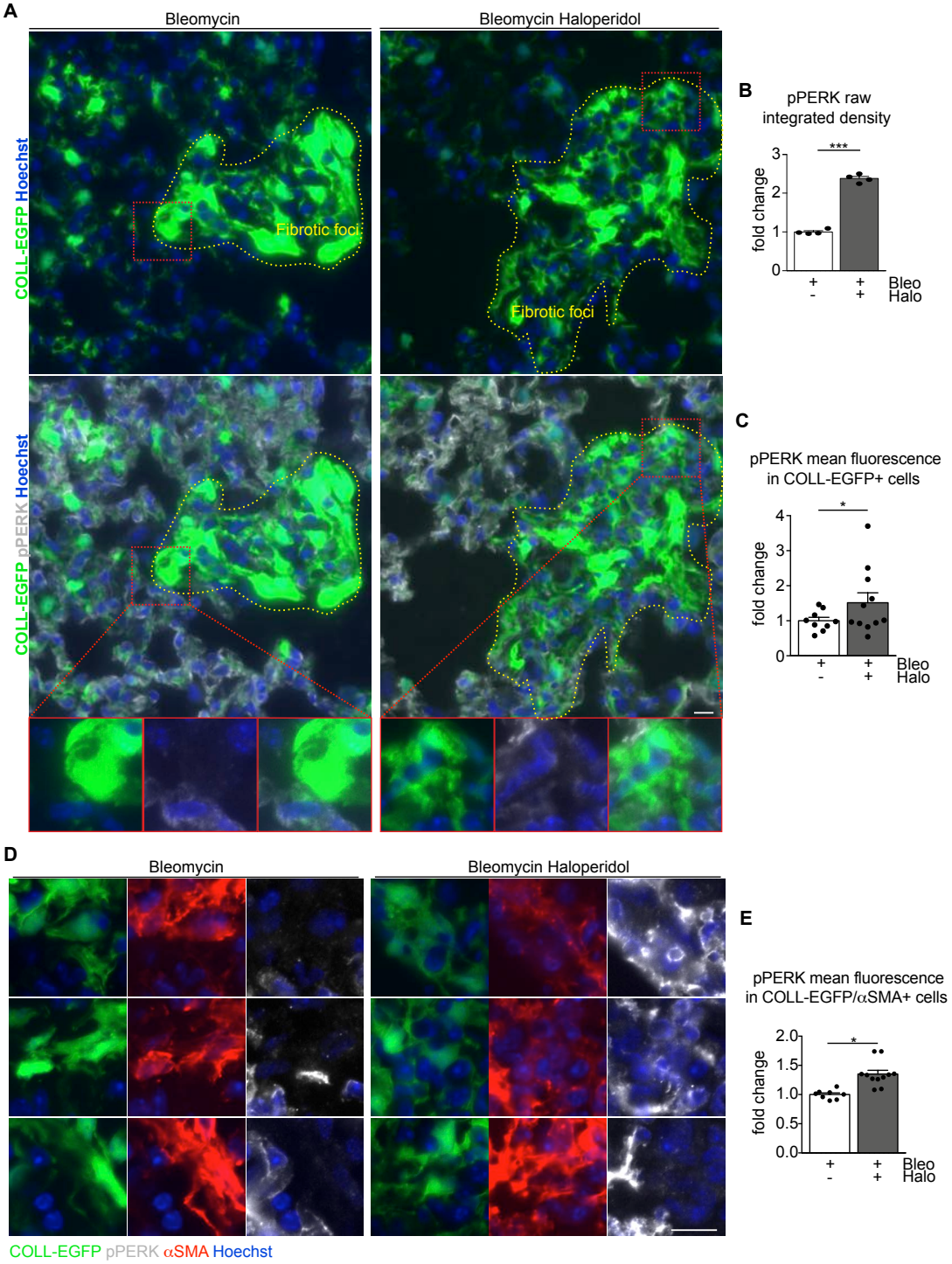

Supplementary Figure 16. **Modulation of ER stress in vivo by Haloperidol.** (**A**) Representative images of lung sections of COLL-EGFP mice exposed to Bleomycin either in the presence or in the absence of Haloperidol and stained with pPERK antibodies (white). Fibrotic foci are indicated by the dashed, yellow line. Nuclei are stained in blue with Hoechst. The lower panels show high magnification of the inset area. (**B**) Raw integrated density of fluorescence intensity of pPERK normalized to total number of nuclei in mice exposed to Bleomycin and treated with Haloperidol (n = 6/gp). (**C**) Quantification of the pPERK mean fluorescence intensity in COLL-EGFP^{+} fibroblasts of lungs exposed to Bleomycin and treated with Haloperidol. (n >5/gp). (**D**) Representative images of three fields of fibrotic foci in lungs of COLL-EGFP mice exposed to Bleomycin and treated with Haloperidol, upon staining with anti-αSMA and anti-pPERK antibodies. Nuclei are stained in blue with Hoechst. (**E**) Quantification of the pPERK mean intensity in COLL-EGFP^{+} αSMA^{+} fibroblasts of lungs exposed to Bleomycin and treated with Haloperidol (n = 6/gp). Scale bar, 50μm in A,D. Values in B, C and E are mean ± SEM. *P<0.05, ***P<0.001 by unpaired t-test, relative to control.

Supplementary figure 17.

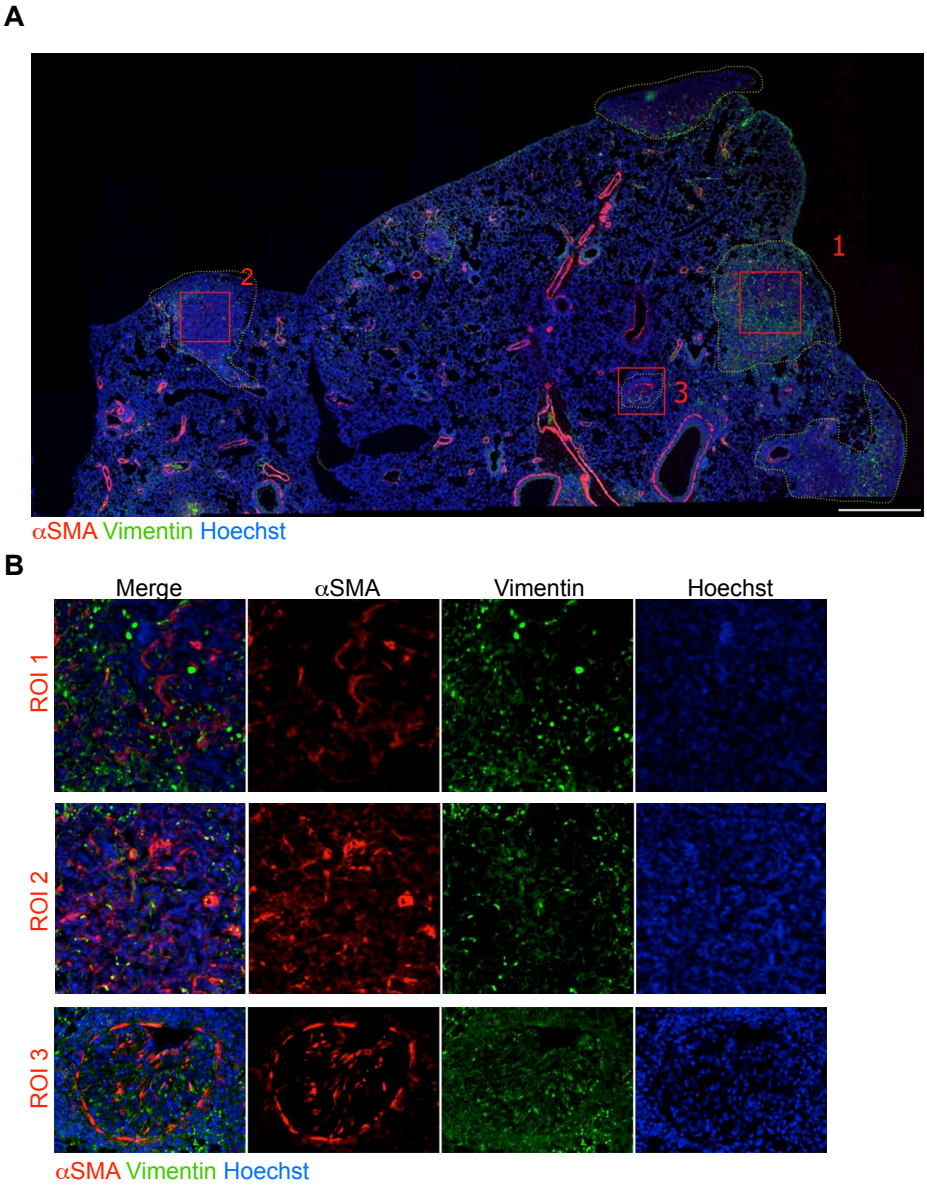

Supplementary Figure 17. Myofibroblasts infiltrate lung cancer. (**A**) Representative section of a tumor-bearing lung at 10 days after LG cell injection, stained with anti-αSMA antibodies in red and anti-vimentin antibodies in green. Nuclei are stained in blue with Hoechst. Tumor foci are shown by the dotted, yellow line. (**B**) High magnification details of the three regions of interests (ROIs) indicated as red squares in A. Scale bar, 1 mm.

Supplementary figure 18.

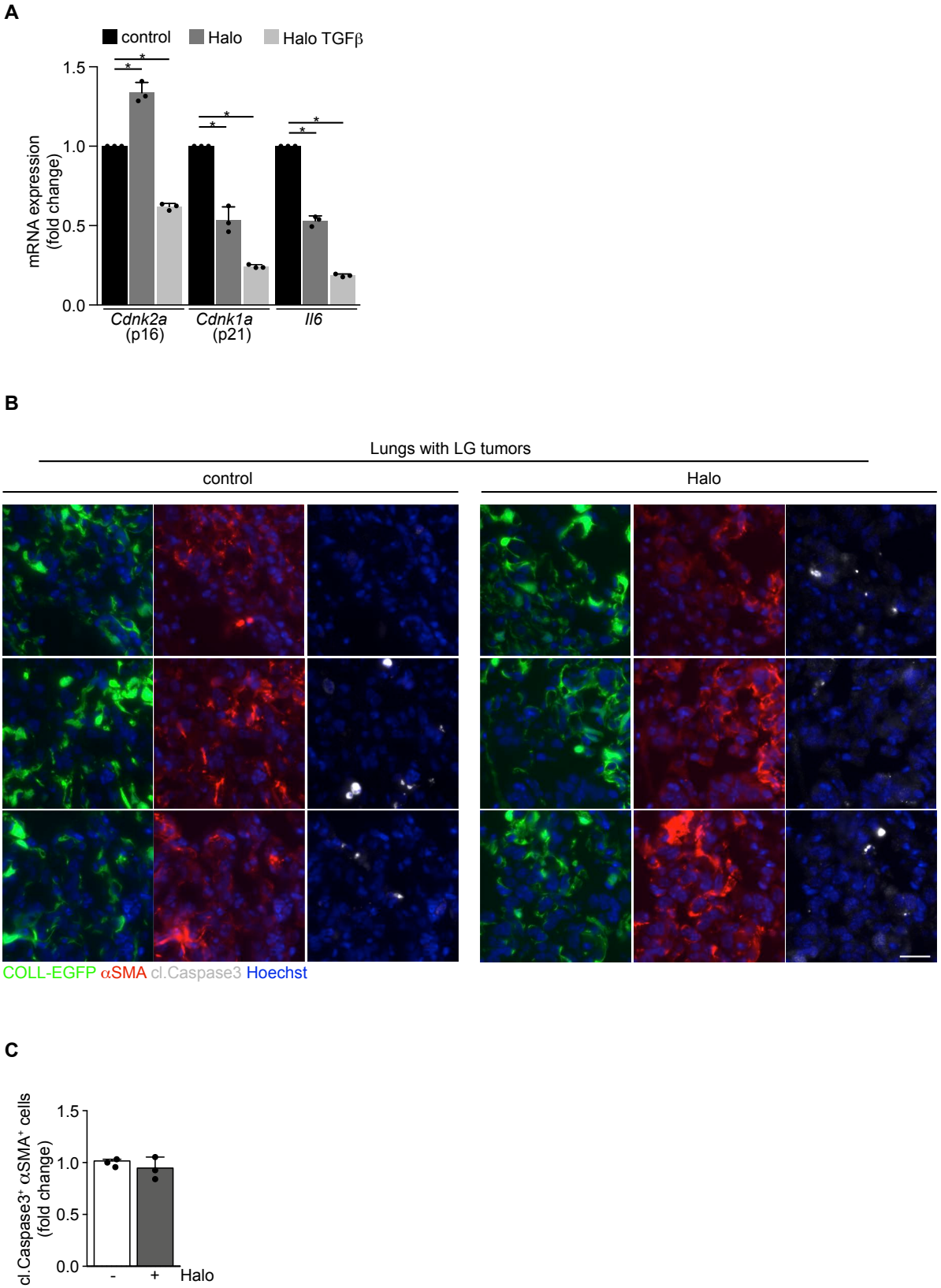

Supplementary Figure 18. Haloperidol does not increase senescence and apoptosis markers. (**A**) Quantification of the mRNA expression of the *Cdkn2a* (p16), *Cdkn1a* (p21) and *Il6* after 3 days of treatment with Haloperidol either alone or in combination with TGFβ. (n = 3 / gp). (**B**) Representative images lung cancer sections of COLL-EGFP mice (fibroblasts in green), stained with anti-cleaved Caspase3 (white) and αSMA (red) antibodies, upon treatment with either PBS (control) or Haloperidol (Halo). Scale bar, 50 μm (**C**) Quantification of the number of fibroblasts positive for both cleaved Caspase 3 and αSMA (n=3 / gp). Values in A and C are mean ± SD. *P<0.05 by unpaired t-test.

Supplementary Table 1. Results of the high-throughput screening of FDA-approved compounds able to control fibroblast to myofibroblast differentiation. The table shows the name of each compound with its Chemical Abstracts Service (CAS) number, the total number of cells in the repeat 1 (R1) and 2 (R2), the average αSMA intensity and the corresponding z-score.

Compound	Total Cells R1 field	Total Cells R2 field	Average alpha SMA Cell mean intensity	Zscore Average alpha SMA Cell mean intensity
50-02-2 - Dexamethasone	286	296	217.731	-2.31640936
52-86-8 - Haloperidol HCl	361	361	221.945	-2.22634743
302-79-4 - Retinoic acid	399	412	224.724625	-2.166941072
314-19-2 - Apomorphine r (-)	354	284	225.4895	-2.150594105
10596-23-3 - Clodronate disodium	398	400	232.94775	-1.991195816
78213-63-5 - Piribedil HCl	348	357	235.47975	-1.937081718
53-03-2 - Prednisone	368	300	236.620125	-1.912709536
73573-88-3 - Mevastatin	292	281	238.139875	-1.880229323
79902-63-9 - Simvastatin	247	220	241.0275	-1.818514781
78919-13-8 - Iloprost	314	292	248.852125	-1.651286297
64211-46-7 - Oxiconazole nitrate	400	349	249.030125	-1.647482068
57-83-0 - Progesterone	370	378	250.527875	-1.61547204
41294-56-8 - Alfacalcidol	345	372	250.929375	-1.606891151
514-78-3 - Canthaxanthin	463	423	252.22175	-1.579270414
66085-59-4 - Nimodipine	342	359	253.129125	-1.559877926
25122-46-7 - Clobetasol propionate	295	250	254.634	-1.527715623
22204-24-6 - Pyrantel pamoate	332	402	257.5285	-1.465854147
22260-51-1 - Bromocriptine mesylate	418	398	259.2795	-1.428431641
123948-87-8 - Topotecan	227	247	259.705875	-1.419319122
154598-52-4 - Efavirenz	364	373	260.6285	-1.39960071
124-94-7 - Triamcinolone	276	251	260.929625	-1.393165044
79855-88-2 - Trequinsin	353	386	261.11525	-1.389197852
31879-05-7 - Fenoprofen	380	410	261.177125	-1.387875455
58-32-2 - Dipyridamole	320	334	261.873625	-1.372989804
67227-56-9 - Fenoldopam mesylate	364	341	262.475625	-1.360123814
55528-07-9 - Butaclamol (+)	431	392	262.609625	-1.357259955
2114454 - Camptothecin	249	226	262.90325	-1.350984579
50-22-6 - Corticosterone	300	221	262.91775	-1.350674684
75330-75-5 - Lovastatin	241	230	263.201625	-1.344607686
61477-96-1 - Piperacillin	394	355	263.900125	-1.329679291
6980-18-3 - Kasugamycin	381	297	264.460875	-1.317694899
11018-89-6 - Ouabain	503	483	265.181125	-1.302301661
28822-58-4 - Isobutylmethylxanthine	492	496	265.53975	-1.2946371
17230-88-5 - Danazol	411	261	265.725625	-1.290664565
82586-55-8 - Quinapril HCl	503	440	268.3335	-1.234928861
50-03-3 - Hydrocortisone 21-acetate	285	243	268.623875	-1.228722945
59052-16-3 - Nalbuphine HCl	474	451	268.65725	-1.228009651
24730-10-7 - Dihydroergocristine mesylate	362	393	269.65375	-1.206712377
120092-68-4 - Manidipine	428	465	269.901	-1.201428131
50-24-8 - Prednisolone	321	289	270.21475	-1.194722642
153559-49-0 - Bexarotene	447	465	270.383875	-1.19110809

54527-84-3 - Nicardipine	451	347	270.503375	-1.188554127
63659-19-8 - Betaxolol HCl	450	397	270.9055	-1.179959881
78613-35-1 - Amorolfine	483	540	271.983125	-1.156928797
19356-17-3 - Calcifediol	255	295	272.087375	-1.154700758
57149-07-2 - Naftopidil 2HCl	360	348	273.41325	-1.126364056
19453 - Galanthamine HBr	499	403	273.718375	-1.119842901
49745-95-1 - Dobutamine HCl	397	352	274.05225	-1.112707299
62929-91-3 - Procaterol hcl	408	440	274.128875	-1.111069664
1400-61-9 - Nystatin	406	349	274.70175	-1.098826135
10118-90-8 - Minocycline HCl	408	310	274.747625	-1.097845691
101975-10-4 - Zardaverine	545	487	274.9085	-1.094407459
49562-28-9 - Fenofibrate	389	361	277.330625	-1.042641618
110871-86-8 - Sparfloxacin	381	398	277.60125	-1.0368578
38776-75-9 - Rifampicin	492	464	278.30225	-1.021875974
2919-66-6 - Melengestrol acetate	277	258	278.42725	-1.019204464
60-56-0 - Methimazole	393	341	278.649125	-1.014462535
183321-74-6 - Erlotinib	333	291	278.666	-1.014101881
33419-42-0 - Etoposide	244	248	279.456375	-0.997209926
107753-78-6 - Zafirlukast	443	427	279.608875	-0.993950685
51-83-2 - Carbamylcholine Cl	474	442	279.70975	-0.991794776
136310-93-5 - Tiotropium Br	345	373	279.760125	-0.990718158
34911-55-2 - Amfebutamone	441	391	280.20875	-0.98113011
568-72-9 - Tanshinone iia	487	466	282.4285	-0.933689444
58186-27-9 - Idebenone	341	298	282.69025	-0.928095303
85760-74-3 - Quinpirole HCl (-)-	423	419	282.850375	-0.924673099
115256-11-6 - Dofetilide	492	416	282.91875	-0.923211783
54350-48-0 - Etretinate	387	348	283.302625	-0.915007577
106017-08-7 - Rufloxacin	337	344	283.699625	-0.906522863
835-31-4 - Naphazoline HCl	345	277	284.090125	-0.898177067
79547-78-7 - Levocabastine HCl	397	378	284.2375	-0.895027357
38304-91-5 - Minoxidil	469	450	284.25275	-0.894701433
134308-13-7 - Tolcapone	372	404	284.393375	-0.891695985
39562-70-4 - Nitrendipine	423	398	284.594625	-0.887394854
130636-43-0 - Nifekalant HCl	367	318	285.11025	-0.876374878
50-07-7 - Mitomycin c	265	278	285.157375	-0.875367718
530-78-9 - Flufenamic acid	427	369	285.181	-0.874862803
53164-05-9 - Acemetacin	383	298	285.201875	-0.874416661
54-85-3 - Isoniazid	448	442	286.275625	-0.851468394
33386-08-2 - Buspirone HCl	357	356	286.29375	-0.851081025
19216-56-9 - Prazosin HCl	319	321	286.30325	-0.85087799
60-31-1 - Acetylcholine Cl	401	348	286.34375	-0.850012421
379-79-3 - Ergotamine D-tartrate	302	328	286.353625	-0.849801372
51022-77-6 - Etazolate	360	412	286.509875	-0.846461985
98319-26-7 - Finasteride	350	297	286.89375	-0.838257779
14611-51-9 - Selegiline	432	417	287.192	-0.831883557
11032-41-0 - Dihydroergotamine mesylate	329	350	287.24925	-0.830660006
6090-95-5 - Conduritol b epoxide	381	388	287.642375	-0.822258108

50-23-7 - Hydrocortisone	336	256	287.664375	-0.821787923
99300-78-4 - Venlafaxine HCl	479	413	287.72525	-0.820486898
39809-25-1 - Penciclovir	400	378	287.795375	-0.818988181
614-39-1 - Procainamide	464	432	287.913125	-0.816471619
75847-73-3 - Enalapril	460	414	287.948375	-0.815718253
132203-70-4 - Cilnidipine	516	430	288.208125	-0.810166856
22254-24-6 - Ipratropium Br	499	432	288.3055	-0.80808575
82640-04-8 - Raloxifene HCl	308	266	288.536125	-0.803156815
82419-36-1 - Ofloxacin	452	378	288.6125	-0.801524523
85371-64-8 - Pinacidil	430	352	289.059	-0.791981891
32222-06-3 - Calcitriol	438	396	289.106125	-0.790974732
103177-37-3 - Pranlukast	432	429	289.585125	-0.780737507
6108-05-0 - Lidocaine	441	423	289.707625	-0.778119428
26807-65-8 - Indapamide	354	366	289.73025	-0.777635884
86386-73-4 - Fluconazole	449	456	289.816875	-0.775784528
99592-32-2 - Sertaconazole	343	397	290.03725	-0.771074657
17360-35-9 - Oxotremorine sesquifumarate	514	451	290.81275	-0.754500612
133-67-5 - Trichloromethiazide	374	340	291.01575	-0.75016208
53885-35-1 - Ticlopidine HCl	410	429	291.34675	-0.743087923
36330-85-5 - Fenbufen	358	317	291.36475	-0.742703225
18046-21-4 - Fentiazac	437	477	291.459375	-0.740680893
42924-53-8 - Nabumetone	316	320	291.779125	-0.733847171
7232-21-5 - Metoclopramide HCl	436	394	291.9875	-0.729393765
3160-91-6 - Moroxydine HCl	524	413	292.051	-0.728036638
81110-73-8 - Racecadotril	478	428	292.404625	-0.720478937
6673-35-4 - Practolol	463	502	292.69625	-0.714246306
826-39-1 - Mecamylamine HCl	415	298	293.007375	-0.707596918
23672-07-3 - Sulpiride s (-)	519	459	293.1335	-0.704901365
73-31-4 - Melatonin	488	430	293.5135	-0.696779976
110429-49-8 - Paroxetine HCl	237	245	293.5395	-0.696224302
NA - Pravastatin lactone	366	302	293.734375	-0.692059419
4205-91-8 - Clonidine HCl	461	400	293.93175	-0.687841105
56-75-7 - Chloramphenicol	435	431	294.156625	-0.683035059
127045-41-4 - Pazufloxacin	432	453	294.678625	-0.671878836
71-82-9 - Levallorphan tartrate	327	335	294.747375	-0.670409505
98-92-0 - Medroxyprogesterone 17-acetate	475	416	294.909375	-0.666947229
84225-95-6 - Raclopride l-tartrate s(-)	479	460	295.30375	-0.658518616
68-96-2 - 17- hydroxyprogesterone	351	381	295.469125	-0.654984209
158966-92-8 - Montelukast	430	387	295.55875	-0.653068737
25812-30-0 - Gemfibrozil	412	460	296.13175	-0.640822537
64-77-7 - Tolbutamide	374	379	296.249	-0.638316661
145-13-1 - Pregnenolone	369	480	296.505125	-0.632842738
149-64-4 - Scopolamine n-butylbromide	393	392	296.56875	-0.631482939
65-49-6 - 4-aminosalicylic acid	417	423	296.580875	-0.631223803
305-03-3 - Chlorambucil	313	334	296.581625	-0.631207774
88671-89-0 - Myclobutanil	444	362	296.68175	-0.629067895
93106-60-6 - Enrofloxacin	405	386	296.8825	-0.624777451

130-61-0 - Thioridazine HCl	295	322	296.970375	-0.622899379
68550-75-4 - Cilostamide	479	395	296.99925	-0.622282261
71125-38-7 - Meloxicam	414	348	297.128375	-0.619522591
73-05-2 - PhentolamineHCl	534	376	297.221625	-0.617529645
63-92-3 - Phenoxybenzamine HCl	465	415	297.340125	-0.614997054
114-80-7 - Neostigmine Br	379	281	297.468375	-0.612256085
363-24-6 - Dinoprostone	328	286	297.536625	-0.610797441
404-86-4 - Capsaicin	319	381	297.62025	-0.609010201
551-11-1 - Dinoprost	483	449	297.72725	-0.606723389
23210-56-2 - Ifenprodil	430	449	297.818375	-0.604775858
91296-87-6 - Sarafloxacin HCl	399	421	297.827875	-0.604572824
5051-62-7 - Guanabenz acetate	384	382	298.15525	-0.59757614
149676-40-4 - Pefloxacine mesylate	451	437	298.230125	-0.595975906
124858-35-1 - Nadifloxacin	297	307	298.36725	-0.59304526
54-92-2 - Iproniazid	393	357	298.42925	-0.591720191
224785-90-4 - Vardenafil	461	434	298.542	-0.58931049
133040-01-4 - Eprosartan	225	252	298.710125	-0.585717309
74863-84-6 - Argatroban	397	463	299.245	-0.57428592
1684-40-8 - Tacrine HCl	417	405	299.63975	-0.565849293
442-51-3 - Harmine	417	375	299.783625	-0.562774385
85721-33-1 - Ciprofloxacin	353	305	300.35475	-0.550568258
24729-96-2 - Clindamycin palmitate	352	365	300.6945	-0.543307095
119-36-8 - Methyl salicylate	453	432	300.800625	-0.541038983
57754-86-6 - Nisoxetine HCl	448	424	300.8965	-0.538989936
378-44-9 - Betamethasone	465	447	300.912625	-0.538645311
2898-76-2 - Benzamil	374	301	300.96125	-0.537606094
2447-57-6 - Sulfadoxine	355	357	300.972625	-0.537362986
170729-80-3 - Aprepitant	319	310	301.02	-0.536350484
58-33-3 - Promethazine HCl	479	456	301.039625	-0.535931057
113806-05-6 - Olopatadine	513	468	301.092375	-0.53480368
111469-81-9 - Naltrindole HCl	436	425	301.14125	-0.53375912
113-92-8 - Chlorpheniramine maleate	331	298	301.15	-0.533572114
1508-75-4 - Tropicamide	348	348	301.165125	-0.533248862
90357-06-5 - Bicalutamide	380	329	301.343125	-0.529444632
40600-13-3 - Cirazoline HCl	419	415	301.627125	-0.523374962
4394-00-7 - Niflumic acid	293	293	302.08675	-0.513551822
50-28-2 - Estradiol	456	375	302.168625	-0.511801983
112965-21-6 - Calcipotriene	479	415	302.235	-0.510383411
2216-88-5 - Ketoprofen (s)	305	334	302.306	-0.508865994
54239-37-1 - Cimaterol	472	408	302.481	-0.50512588
20537-88-6 - Amifostine	477	364	302.521	-0.504270997
114-49-8 - Scopolamine HBr	362	391	302.522	-0.504249625
18683-91-5 - Ambroxol	401	389	302.773875	-0.498866534
68291-97-4 - Zonisamide	264	300	302.926625	-0.495601949
90-69-7 - Lobeline	425	440	302.972	-0.494632191
125494-59-9 - Sibutramine HCl	408	366	303.017125	-0.493667776
04199-10-4 - Propranolol HCl s(-)	344	301	303.119125	-0.491487824

16320-04-0 - Gestrinone	516	484	303.686	-0.479372528
196618-13-0 - Oseltamivir	370	321	303.739625	-0.478226451
58066-85-6 - Miltefosine	443	462	303.84575	-0.475958339
53716-50-0 - Oxfendazole	366	299	303.962125	-0.473471164
103890-78-4 - Lacidipine	381	428	304.148375	-0.469490614
21187-98-4 - Gliclazide	472	452	304.194	-0.468515514
82009-34-5 - Cilastatin	464	363	304.223125	-0.467893052
14252-80-3 - Bupivacaine HCl	445	392	304.39475	-0.464225069
124832-27-5 - Valaciclovir	376	298	304.467375	-0.462672922
50-40-1 - Norepinephrine-(+)-tartrate l (-)	336	335	304.54525	-0.461008572
90098-04-7 - Rebamipide	474	517	304.621875	-0.459370936
56296-78-7 - Fluoxetine HCl	314	257	304.968125	-0.451970855
139755-83-2 - Sildenafil	341	323	304.986625	-0.451575471
100643-71-8 - Desloratadine	370	343	305.0625	-0.449953865
129-46-4 - Suramin sodium	446	406	305.78125	-0.434592685
79-83-4 - Pantothenic acid	315	204	305.8175	-0.433817947
65277-42-1 - Ketoconazole	310	321	305.935125	-0.431304057
69-09-0 - Chlorpromazine HCl	390	366	305.9705	-0.43054802
50-41-9 - Clomiphene citrate	301	293	306.135125	-0.427029642
62893-19-0 - Cefoperazone acid	426	446	306.334375	-0.422771255
64490-92-2 - Tolmetin Na	452	398	306.467875	-0.419918083
151615 - Oxymetazoline HCl	505	401	306.782125	-0.413201908
145781-92-6 - Goserelin acetate	379	337	306.829875	-0.412181391
74050-98-9 - Ketanserin tartrate	348	361	306.970875	-0.409167929
53-86-1 - Indomethacin	359	397	307.032	-0.407861561
3778-73-2 - Ifosfamide	352	305	307.147875	-0.405385071
590-63-6 - Carbamyl-beta-methylcholine Cl	502	461	307.168875	-0.404936258
57808-65-8 - Closantel	376	279	307.767375	-0.39214507
1841-19-6 - Fluspirilene	292	265	307.8335	-0.390731841
59804-37-4 - Tenoxicam	236	220	307.995	-0.387280251
65-29-2 - Gallamine triethiodide	394	361	308.178875	-0.38335046
112809-51-5 - Letrozole	326	369	308.288125	-0.381015561
29122-68-7 - Atenolol	440	370	308.38975	-0.378843624
32672-69-8 - Mesoridazine besylate	295	285	308.97975	-0.366234099
67-73-2 - Fluocinolone acetonide	313	294	309.18175	-0.361916939
59122-46-2 - Misoprostol	425	410	309.191875	-0.361700547
54-71-7 - Pilocarpine HCl	508	529	309.256875	-0.360311362
109889-09-0 - Granisetron	252	282	309.316375	-0.359039723
54143-56-5 - Flecainide	472	426	309.38025	-0.357674582
51-30-9 - Isoproterenol HCl (rac)	380	343	309.4395	-0.356408286
59-33-6 - Mepyramine maleate	356	353	309.601375	-0.352948682
5630-53-5 - Tibolone	350	330	310.27275	-0.338600004
50-12-4 - Mephenytoin	290	373	310.353625	-0.336871537
57076-71-8 - Denbufylline	460	437	310.415125	-0.335557154
3366-95-8 - Secnidazole	396	429	310.551125	-0.332650552
111406-87-2 - Zileuton	465	444	310.55975	-0.332466218
81409-90-7 - Cabergoline	399	313	310.63275	-0.330906056

77883-43-3 - Doxazosin mesylate	338	373	310.69675	-0.329538243
212141-54-3 - Vatalanib	223	205	310.729625	-0.328835636
147536-97-8 - Bosentan	343	368	311.183	-0.319146071
113712-98-4 - Tenatoprazole	382	211	311.240375	-0.317919848
82410-32-0 - Ganciclovir	508	494	311.347625	-0.315627693
53-43-0 - Dehydroepiandrosterone	422	377	311.75625	-0.306894528
119302-91-9 - Rocuronium bromide	440	376	311.77275	-0.306541889
123441-03-2 - Rivastigmine	428	445	311.789	-0.306194593
68-22-4 - Norethindrone	283	214	311.81425	-0.305654948
63-45-6 - Primaquine phosphate	304	295	311.837875	-0.305150033
105956-99-8 - Clinafloxacin HCl	313	299	311.89	-0.304036013
106266-06-2 - Risperidone	384	330	312.010875	-0.301452663
69004-03-1 - Toltrazuril	403	315	312.033875	-0.300961106
169590-42-5 - Celecoxib	408	422	312.097625	-0.299598636
18378-89-7 - Plicamycin	241	238	312.173	-0.297987715
5786-21-0 - Clozapine	449	367	312.213875	-0.297114132
40391-99-9 - Pamidronic acid	305	239	312.23025	-0.296764164
1421-86-9 - Strychnine HCl	505	392	312.724	-0.286211701
15826-37-6 - Disodium cromoglycate	424	371	312.873125	-0.28302459
2016-88-8 - Amiloride	431	364	313.01025	-0.280093944
541-22-0 - Decamethonium 2Br	362	290	313.1585	-0.276925534
105816-04-4 - nateglinide	443	391	313.27925	-0.274344856
64221-86-9 - Imipenem	355	315	313.617375	-0.267118423
57381-26-7 - Irsogladine maleate	467	457	313.67775	-0.265828083
82571-53-7 - Ozagrel	234	278	313.73675	-0.264567131
72509-76-3 - Felodipine	301	303	314.00775	-0.258775298
154-21-2 - Lincomycin	400	324	314.266625	-0.253242602
595-33-5 - Megestrol acetate	401	343	314.4635	-0.249034974
147221-93-0 - Delavirdine mesylate	413	422	314.501875	-0.248214821
51-21-8 - 5-fluorouracil	375	319	314.555125	-0.247076758
90-05-1 - Guaiacol	432	463	314.5655	-0.246855023
5104-49-4 - Flurbiprofen	454	456	314.649625	-0.245057097
74011-58-8 - Enoxacin	404	382	314.694	-0.244108711
21829-25-4 - Nifedipine	318	324	314.739625	-0.24313361
26921-17-5 - Timolol maleate (s)	413	435	315.011125	-0.237331091
16676-29-2 - Naltrexone HCl	339	398	315.134875	-0.234686297
112529-15-4 - Pioglitazone	391	401	315.312875	-0.230882067
1166-34-3 - Cinanserin	362	348	315.375625	-0.229540969
63527-52-6 - Cefotaxime acid	434	443	315.385125	-0.229337934
51322-75-9 - Tizanidine HCl	393	279	315.424	-0.228507095
51803-78-2 - Nimesulide	390	346	315.4965	-0.226957619
21462-39-5 - Clindamycin HCl	405	338	315.868625	-0.219004535
357-08-4 - Naloxone HCl	442	413	316.12525	-0.213519926
93479-97-1 - Glimepiride	385	432	316.223	-0.211430806
60628-96-8 - Bifonazole	453	450	316.4265	-0.207081588
53902-12-8 - Tranilast	427	468	316.874625	-0.197504227
51022-70-9 - Salbutamol sulfate	466	465	317.52875	-0.183524217

84371-65-3 - Mifepristone	274	279	317.766375	-0.178445677
63968-64-9 - Artemisinin	416	396	318.048625	-0.172413409
60-54-8 - Tetracycline	460	352	318.16075	-0.170017065
78415-72-2 - Milrinone	508	436	318.177	-0.169669768
19728-88-2 - Methiothepin maleate	261	271	318.395	-0.165010656
104632-26-0 - Pramipexole	361	332	318.499125	-0.162785288
5536-17-4 - Vidarabine	452	443	318.812	-0.1560985
37762-06-4 - Zaprinast	563	445	319.04925	-0.151027975
51037-30-0 - Acipimox	411	396	319.105375	-0.149828467
88150-42-9 - Amlodipine	514	463	319.126875	-0.149368967
120279-95-0 - Dorzolamide	263	304	319.164	-0.148575529
1405-54-5 - Tylosin tartrate	387	366	319.43925	-0.142692865
99-66-1 - Valproic acid	522	483	319.715	-0.136799515
2068-78-2 - Vincristine sulfate	439	434	319.7315	-0.136446876
148-82-3 - Melphalan	264	241	319.957125	-0.131624801
749-02-0 - Spiperone	451	417	320.0515	-0.129607811
100490-36-6 - Tosufloxacin	322	241	320.128125	-0.127970176
114-70-5 - Sodium phenylacetate	255	286	320.190125	-0.126645107
57-41-0 - Phenytoin	461	400	320.38475	-0.122485567
28721-07-5 - Oxcarbazepine	367	336	320.726375	-0.115184331
57-94-3 - Tubocurarine Cl (+)	485	462	320.758875	-0.114489739
143491-57-0 - Emtricitabine	560	511	320.83325	-0.11290019
6119-47-7 - Quinine	521	411	320.854	-0.11245672
959-24-0 - Sotalol HCl	455	479	320.86075	-0.112312458
36322-90-4 - Piroxicam	422	364	320.927	-0.110896558
60142-96-3 - Gabapentin	540	502	320.943	-0.110554605
78110-38-0 - Aztreonam	491	483	321.166	-0.105788632
102767-28-2 - Levetiracetam	439	402	321.381125	-0.101190964
104227-87-4 - Famciclovir	388	409	321.417	-0.100424241
93793-83-0 - Roxatidine acetate HCl	480	381	321.4405	-0.099921997
88495-63-0 - Artesunate	266	241	321.469125	-0.099310221
89197-32-0 - Efaroxan	391	267	321.506	-0.098522126
22494-42-4 - Diflunisal	394	351	322.102625	-0.085771011
3506-09-0 - Propranolol	294	352	322.2255	-0.083144917
50-35-1 - Thalidomide	270	245	322.274	-0.082108371
52549-17-4 - Pranoprofen	450	440	322.573375	-0.075710106
1791337 - Carbadox	460	415	322.594125	-0.075266635
2038-35-9 - Phenamil	519	480	322.617125	-0.074775077
36791-04-5 - Ribavirin	383	414	322.784875	-0.071189912
436349 - Doxifluridine	376	256	322.825	-0.070332357
120511-73-1 - Anastrozole	372	411	323.018625	-0.066194189
52-01-7 - Spironolactone	271	298	323.159875	-0.063175383
62658-64-4 - Bopindolol malonate	251	244	323.512375	-0.055641726
97825-25-7 - Ractopamine	366	335	323.514375	-0.055598982
139481-59-7 - Candesartan	301	428	323.645625	-0.052793897
152459-95-5 - Imatinib	229	206	323.695875	-0.05171995
81-24-3 - Taurocholic acid, sodium salt hydrate	375	393	323.751625	-0.050528457

7414-83-7 - Etidronate 2Na	477	351	323.88325	-0.047715357
74764-40-2 - Bepridil	377	298	323.958125	-0.046115123
15500-66-0 - Pancuronium Br	414	407	324.001125	-0.045196124
159989-64-7 - Nelfinavir Mesylate	309	317	324.037	-0.0444294
112964-99-5 - Hydroxytacrine maleate	473	457	324.052875	-0.044090119
63675-72-9 - Nisoldipine	281	283	324.1225	-0.042602088
72656-09-3 - Carvedilol	320	293	324.2635	-0.039588625
80288-49-9 - Furafylline	414	373	324.2665	-0.039524509
72432-10-1 - Aniracetam	296	327	324.581	-0.032802991
603-50-9 - Bisacodyl	474	497	324.68875	-0.03050015
54-31-9 - Furosemide	454	448	324.713875	-0.029963176
143-67-9 - Vinblastine sulfate	484	441	324.787625	-0.028386986
50-91-9 - Floxuridine	328	304	324.81725	-0.027753838
6998-60-3 - Rifamycin sv	345	265	325.099875	-0.021713555
103745-39-7 - Fasudil	435	399	325.192625	-0.019731295
73210-73-8 - Xamoterol hemifumarate	479	502	325.204875	-0.019469487
566-48-3 - Formestane	335	367	325.21125	-0.01933324
69975-86-6 - Doxofylline	458	418	325.44975	-0.014235999
2058-52-8 - Clothiapine	421	424	325.897625	-0.004663981
85622-93-1 - Temozolomide	409	307	326.164625	0.001042364
66104-23-2 - Pergolide mesylate	429	384	326.17275	0.001216012
34580-14-8 - Ketotifen fumarate	408	374	326.276375	0.003430693
13710-19-5 - Tolfenamic acid	455	367	327.2605	0.024463488
38194-50-2 - Sulindac	489	471	327.54375	0.030517129
144689-63-4 - Olmesartan	448	477	327.67475	0.033316871
101477-55-8 - Lomerizine HCl	304	240	327.921	0.038579745
50700-72-6 - Vecuronium Br	312	279	328.201875	0.044582627
1951-25-3 - Amiodarone	294	245	328.267	0.045974483
24390-14-5 - Doxycycline HCl	442	417	328.497125	0.050892732
2963-78-2 - Butyrylcholine Cl	451	445	328.561375	0.052265888
83366-66-9 - Nefazodone	323	324	328.651625	0.054194718
103628-48-4 - Sumatriptan Succinate	358	388	328.724875	0.055760222
70458-96-7 - Norfloxacin	388	389	328.76425	0.056601748
1156-19-0 - Tolazamide	434	490	329.0965	0.06370262
135046-48-9 - Clopidogrel sulfate	229	293	329.293	0.067902233
79944-56-2 - Idazoxan	383	386	329.508875	0.07251593
161814-49-9 - Amprenavir	369	387	329.58125	0.074062734
14028-44-5 - Amoxapine	496	455	329.622875	0.074952347
67121-76-0 - Fluperlapine	420	375	329.7885	0.078492097
105462-24-6 - Risedronic acid	384	286	329.81375	0.079031742
7481-89-2 - 2',3' - dideoxycytidine	498	418	330.28975	0.089204851
132-98-9 - Pencillin v potassium	409	414	330.317375	0.089795254
298-46-4 - Carbamazepine	372	386	330.782375	0.09973327
93-14-1 - Guaifenesin	421	433	331.153375	0.10766231
81103-11-9 - Clarithromycin	306	254	331.269125	0.110136128
21736-83-4 - Spectinomycin	408	329	331.597375	0.117151512
100986-85-4 - Levofloxacin HCl	289	212	331.73175	0.120023385

73220-03-8 - Remoxipride	458	477	331.866875	0.122911287
364-98-7 - Diazoxide	502	454	332.309625	0.132373774
146-48-5 - Yohimbine HCl	427	406	332.360875	0.133469092
87333-19-5 - Ramipril	443	445	332.401	0.134326647
636-54-4 - Clopamide	353	338	332.826	0.14340978
113-52-0 - Imipramine HCl	412	388	332.952625	0.146116019
29094-61-9 - Glipizide	349	321	333.002625	0.147184623
54029-12-8 - Ricobendazole	444	431	333.032875	0.147831128
146-56-5 - Fluphenazine 2HCl	281	271	333.1015	0.149297787
54-42-2 - Idoxuridine	234	225	333.148125	0.15029426
80809-81-0 - Docebenone	246	283	333.294125	0.153414583
80214-83-1 - Roxithromycin	439	399	333.35425	0.154699579
7177-48-2 - Ampicillin trihydrate	462	483	333.3785	0.155217852
28797-61-7 - Pirenzepine 2HCl	342	393	333.43825	0.156494833
72558-82-8 - Ceftazidime	411	447	333.813375	0.164512034
10347-81-6 - Maprotiline HCl	384	313	333.84875	0.165268071
202409-33-4 - Etoricoxib	386	335	334.460125	0.178334424
147-24-0 - Diphenhydramine HCl	523	443	335.2495	0.195205007
79660-72-3 - Fleroxacin	476	416	335.885	0.208786961
129722-12-9 - Aripiprazole	354	379	336.01225	0.211506558
13523-86-9 - Pindolol	427	387	336.327375	0.218241434
59277-89-3 - Acycloguanosine	436	370	336.344625	0.218610102
37148-27-9 - Clenbuterol	430	438	336.4175	0.220167592
184475-35-2 - Gefitinib	281	247	336.457875	0.22103049
532-11-6 - Anethole-trithione (anetholtrithion)	316	335	336.5175	0.2223048
115956-12-2 - Dolasetron	281	351	336.578625	0.223611168
1054-88-2 - Spiroxatrine	423	431	336.657625	0.225299562
28395-03-1 - Bumetanide	360	382	336.73825	0.227022686
83150-76-9 - Octreotide	366	331	336.876625	0.229980047
162011-90-7 - Rofecoxib	411	358	337.0855	0.234444139
84057-84-1 - Lamotrigine	360	423	337.104875	0.234858223
111974-72-2 - Quetiapine fumarate	444	380	337.29225	0.238862816
62571-86-2 - Captopril	256	240	337.416625	0.241520968
443-48-1 - Metronidazole	366	338	337.47175	0.242699104
23313-68-0 - Verapamil	422	386	337.502625	0.243358967
51-40-1 - Epinephrine-(+)-tartrate l (-)	417	430	337.73275	0.248277216
13707-88-5 - Alprenolol HCl	472	377	337.8765	0.251349452
27203-92-5 - Tramadol HCl	392	355	338.085625	0.255818887
361-37-5 - Methysergide	297	314	338.14875	0.257167999
68373-14-8 - Sulbactam	431	388	338.293125	0.260253593
1405-10-3 - Neomycin sulfate	301	303	338.58525	0.266496911
41859-67-0 - Bezafibrate	535	522	338.80475	0.271188082
555-30-6 - Methyldopa	394	345	338.936625	0.274006524
517- 89- 5 - Shikonin	436	422	338.96425	0.274596928
56392-17-7 - Metoprolol tartrate	369	284	339.09	0.277284466
66357-59-3 - Ranitidine HCl	492	446	339.122	0.277968373
13311-84-7 - Flutamide	524	431	339.761875	0.29164383

54965-24-1 - Tamoxifen citrate	267	247	339.923375	0.295095421
59865-13-3 - Cyclosporin a	406	313	340.049125	0.297782959
891986 - Dacarbazine	303	207	340.054875	0.297905849
2078-54-8 - Propofol	293	333	340.12025	0.299303048
1677687 - Pentoxifylline	438	361	340.27375	0.302583662
14222-60-7 - Prothionamide	429	436	340.323125	0.303638908
30516-87-1 - 3'-azido-3'-deoxythymidine	459	436	340.4865	0.307130571
315-30-0 - Allopurinol	476	428	340.91	0.316181646
745-65-3 - Alprostadil	386	399	341.008375	0.318284124
65141-46-0 - Nicorandil	454	401	341.16375	0.32160481
51-02-5 - Pronethalol HCl	479	469	341.380375	0.326234536
50-27-1 - Estriol	418	375	341.380625	0.326239879
7240-38-2 - Oxacillin sodium monohydrate	409	360	341.4	0.326653963
70288-86-7 - Ivermectin	400	417	341.62225	0.331403907
306-40-1 - Succinylcholine	260	249	342.305625	0.34600905
59-92-7 - Levodopa	332	272	342.401875	0.348066112
611-75-6 - Bromhexine HCl	472	452	342.510375	0.350384982
84625-61-6 - Itraconazole	350	360	343.25975	0.366400682
73590-58-6 - Omeprazole	337	333	343.869	0.37942162
57773-63-4 - Triptorelin	395	280	344.218375	0.386888489
98079-52-8 - Lomefloxacin HCl	288	256	344.313375	0.388918836
129453-61-8 - Fulvestrant	267	295	344.487	0.392629563
92623-83-1 - Pravadoline	448	401	344.843	0.400238022
1405-41-0 - Gentamycin sulfate	489	452	345.300375	0.410013076
57808-66-9 - Domperidone	392	368	346.41075	0.433744095
71751-41-2 - Abamectin	363	363	346.840125	0.44292073
581-88-4 - Debrisoquin sulfate	274	270	347.246375	0.451603137
81732-65-2 - Bambuterol	449	451	347.463125	0.456235534
10418-03-8 - Stanozolol	318	301	347.688	0.46104158
315-80-0 - Dibenzepine HCl	440	422	347.713375	0.461583896
13010-47-4 - Lomustine	307	295	347.721125	0.46174953
102625-70-7 - Pantoprazole	429	374	347.966875	0.467001718
427-51-0 - Cyproterone acetate	297	283	348.055375	0.468893146
637-07-0 - Clofibrate	324	296	348.1935	0.471845164
53-16-7 - Estrone	395	323	348.2645	0.473362582
111555-58-9 - Naltriben mesylate	412	438	348.411625	0.476506949
69655-05-6 - Didanosine	361	442	348.436625	0.477041251
121268-17-5 - Alendronate	401	342	348.955875	0.488138701
64795-35-3 - Mesulergine HCl	424	438	349.08325	0.490860969
64228-81-5 - Atracurium besylate	356	337	349.112375	0.491483431
645-05-6 - Altretamine	447	397	349.345	0.49645511
440-17-5 - Trifluoperazine	320	286	350.03975	0.511303361
144701-48-4 - Telmisartan	288	293	350.406875	0.519149584
58-54-8 - Ethacrynic acid	320	379	350.41025	0.519221715
3521-84-4 - Meglumine	475	372	350.572	0.522678648
63590-64-7 - Terazosin HCl	270	300	350.596	0.523191578
95635-56-6 - Ranolazine 2HCl	472	447	350.6745	0.524869286

78755-81-4 - Flumazenil	267	257	351.43125	0.541042605
76824-35-6 - Famotidine	514	475	351.432625	0.541071992
130929-57-6 - Entacapone	257	349	352.241875	0.558367344
115344-47-3 - Siguazodan	481	395	352.575375	0.565494932
2971-90-6 - Clopidol	253	283	352.82175	0.570760477
105826-92-4 - Tropisetron HCl	417	363	352.82425	0.570813908
130209-82-4 - Latanoprost	409	390	352.845	0.571257378
96036-03-2 - Meropenem	362	337	352.891	0.572240494
50847-11-5 - Ibudilast	364	212	353.192375	0.578681503
1986-47-6 - Tranylcypromine	455	322	353.235875	0.579611188
21535-47-7 - Mianserin hcl	359	286	353.353375	0.582122407
99464-64-9 - Ampiroxicam	428	421	353.470625	0.584628283
60-81-1 - Phloridzin	287	208	353.6885	0.589284725
6138-79-0 - Trans-triprolidine HCl	432	421	353.753625	0.590676581
14838-15-4 - Phenylpropanolamine	326	254	354.107	0.598228939
64-47-1 - Physostigmine sulfate	388	374	354.11625	0.59842663
122892-31-3 - Itopride HCl	370	381	354.5345	0.607365501
55268-74-1 - Praziquantel	403	376	354.6915	0.610720917
322-35-0 - Benserazide HCl	367	325	355.19575	0.621497787
388082-78-8 - Lapatinib	300	283	355.929625	0.637182219
366-70-1 - Procarbazine HCl	517	406	356.185625	0.642653471
1649-18-9 - Azaperone	550	454	356.202625	0.643016796
3810-74-0 - Streptomycin sulfate	329	306	356.31775	0.645477257
81147-92-4 - Esmolol	287	263	357.423625	0.669112102
50-33-9 - Phenylbutazone	452	404	358.684875	0.696067633
54063-53-5 - Propafenone	485	473	358.7725	0.697940361
657-24-9 - Metformin	427	329	358.950125	0.701736576
119141-88-7 - Esomeprazole potassium	418	401	359.064125	0.704172993
15687-27-1 - Ibuprofen	298	251	359.54475	0.714444947
95734-82-0 - Nedaplatin	303	320	359.916625	0.722392688
54187-04-1 - Rilmenidine hemifumarate	411	431	360.020625	0.724615384
34552-83-5 - Loperamide	262	251	360.07625	0.725804206
51-12-7 - Nialamide	341	352	360.1895	0.728224594
91161-71-6 - Terbinafine HCl	412	292	360.436375	0.733500825
15307-79-6 - Diclofenac,Na	375	362	360.953375	0.744550189
73231-34-2 - Florfenicol	416	371	361.034875	0.746292013
7361-61-7 - Xylazine HCl	414	432	361.152875	0.748813918
165800-03-3 - Linezolid	533	464	361.491625	0.756053709
128196-01-0 - Escitalopram	278	290	362.43	0.776108731
1716-12-7 - Sodium phenylbutyrate	367	288	362.632125	0.780428562
88040-23-7 - Cefepime	365	379	362.803375	0.78408853
99614-01-4 - Ondansetron	402	395	363.615875	0.801453342
83905-01-5 - Azithromycin	486	450	363.733875	0.803975247
42971-09-5 - Vinpocetine	265	368	364.19725	0.813878533
25717-80-0 - Molsidomine	501	482	364.74125	0.825504943
41575-94-4 - Carboplatin	453	479	364.94625	0.829886218
19982-08-2 - Memantine HCl	334	325	365.736875	0.846783516

28860-95-9 - Carbidopa	351	315	365.97825	0.851942201
6055-19-2 - Cyclophosphamide monohydrate	372	314	366.216875	0.857042113
97322-87-7 - Troglitazone	461	391	366.94925	0.872694487
483-63-6 - Crotamiton	327	322	366.988625	0.873536013
14976-57-9 - Clemastine fumarate	307	323	367.4565	0.883535473
118072-93-8 - Zoledronic acid	335	265	367.821375	0.89133361
55-48-1 - Atropine sulfate	430	355	367.907625	0.893176951
147416-96-4 - Telenzepine 2HCl	411	338	368.317	0.901926145
37321-09-8 - Apramycin	438	413	368.718	0.910496348
38083-17-9 - Climbazole	270	290	368.778625	0.91179203
41570-61-0 - Tulobuterol	360	363	369.106375	0.918796728
22204-53-1 - Naproxen	309	372	369.289625	0.922713161
125-84-8 - Dl-aminoglutethimide	520	429	369.394375	0.924951886
64224-21-1 - Oltipraz	459	411	370.474125	0.948028385
124750-99-8 - Losartan potassium	235	229	370.967375	0.958570162
26786-84-5 - Lomofungin	480	426	371.236	0.964311236
84-16-2 - Hexestrol	375	403	371.261125	0.96484821
68475-42-3 - Anagrelide	396	359	371.599875	0.972088
1501-84-4 - Rimantadine HCl	408	419	371.740875	0.975101463
32828-81-2 - Picotamide	405	455	372.06275	0.9819806
749-13-3 - Trifluperidol 2HCl	257	205	372.141875	0.983671666
112811-59-3 - Gatifloxacin	427	459	372.52575	0.991875872
56-53-1 - Diethylstilbestrol	341	346	372.6685	0.994926736
122-11-2 - Sulfadimethoxine	334	340	372.778	0.997266978
976-71-6 - Canrenone	428	442	372.94425	1.000820086
CTRL	364.015625	331.375	373.1361279	1.004920916
128794-94-5 - Mycophenolate mofetil	344	292	373.49675	1.012628158
35898-87-4 - Dilazep	439	426	374.182125	1.027276045
1744-22-5 - Riluzole HCl	237	268	374.624375	1.036727846
302-22-7 - Chlormadinone acetate	377	405	375.12075	1.04733641
434-03-7 - Ethisterone	477	474	375.379375	1.052863763
16170-76-6 - Bromebric acid	445	444	376.543	1.077732846
35208-55-0 - Clindamycin PO4	391	373	377.035875	1.088266608
60607-34-3 - Oxatomide	461	445	377.558625	1.099438861
2062-78-4 - Pimozide	246	232	377.756375	1.103665189
27848-84-6 - Nicergoline	434	403	377.9525	1.107856788
22071-15-4 - Ketoprofen	345	289	378.341875	1.11617854
14611-52-0 - Deprenyl HCl r (-)	383	334	378.411625	1.117669242
21498-08-8 - Lofexidine	370	313	379.29075	1.136457969
317-34-0 - Aminophylline	416	290	379.390375	1.138587162
61413-54-5 - Rolipram	453	425	379.9025	1.149532337
497-30-3 - Ergothioneine	479	405	380.398625	1.160135558
2393-92-2 - Thiamphenicol glycinate	465	378	380.5045	1.162398327
19387-91-8 - Tinidazole	325	279	382.332375	1.201463811
114084-78-5 - Ibandronate	398	341	382.361	1.202075587
99011-02-6 - Imiquimod	342	312	383.3785	1.223821675
30484-77-6 - Flunarizine-2HCl	346	356	385.194875	1.26264138

50-78-2 - Acetylsalicylic acid	477	376	386.758375	1.296056621
10238-21-8 - Glyburide	408	389	387.647375	1.315056397
139264-17-8 - zolmitriptan	302	270	389.07575	1.345583737
123318-82-1 - Clofarabine	447	430	389.263375	1.349593673
95233-18-4 - Atovaquone	331	354	389.377875	1.352040776
72599-27-0 - Miglustat	361	423	389.6425	1.357696361
114977-28-5 - Docetaxil	290	257	390.4715	1.375413813
59729-33-8 - Citalopram	341	274	391.433375	1.395971079
68-26-8 - Vitamin a (acetate)	408	378	392.214875	1.412673357
69014-14-8 - Tiotidine	340	304	394.02675	1.451396888
16595-80-5 - Levamisole HCl	311	306	394.147875	1.45398558
738-70-5 - Trimethoprim	367	341	394.272	1.456638389
106463-17-6 - Tamsulosin HCl	316	264	394.994625	1.472082386
22916-47-8 - Miconazole	339	310	395.113625	1.474625663
76420-72-9 - Enalaprilat	390	304	395.465875	1.482153977
50-63-5 - Chloroquine phosphate	357	330	395.885125	1.49111422
32986-56-4 - Tobramycin (free base)	311	258	397.184125	1.518876548
89-57-6 - 5-aminosalicylic acid	510	488	397.710875	1.530134289
68-35-9 - Sulfadiazine	321	312	397.868125	1.533495048
83915-83-7 - Lisinopril	262	230	398.4515	1.545962983
17902-23-7 - Ftorafur	527	417	399.349125	1.565147093
33286-22-5 - Diltiazem	465	425	400.7805	1.595738549
65899-73-2 - Tioconazole	335	240	400.933375	1.599005805
100-33-4 - Pentamidine	332	350	401.817625	1.617904064
311074 - Troleandomycin	405	299	404.48075	1.674820575
132539-06-1 - Olanzapine	370	377	404.6635	1.678726322
51481-61-9 - Cimetidine	416	379	405.116375	1.688405201
61-68-7 - Mefenamic acid	265	215	413.431625	1.86611936
101828-21-1 - Butenafine	287	306	418.920125	1.983420001
79794-75-5 - Loratadine	232	220	429.030375	2.199497037
89796-99-6 - Aceclofenac	400	358	433.915	2.303891616
1476-53-5 - Novobiocin Na	338	267	443.784	2.514812639
97964-56-2 - Lorglumide	228	230	444.4285	2.528586942
797-63-7 - Levonorgestrel	251	244	445.419125	2.549758655
89365-50-4 - Salmeterol	330	294	448.58375	2.617393263
53123-88-9 - Rapamycin	228	246	453.578625	2.724144113
125-69-9 - Dextromethorphan HBr	398	402	460.928875	2.881234218
31431-39-7 - Mebendazol	243	246	486.422	3.426075235
31430-15-6 - Flubendazole	242	214	493.08225	3.568418607
23110-15-8 - Fumagillone	315	244	698.482	7.958237768

Supplementary Table 2. Detailed description of the interaction between the ligand the receptor.

Ligand		Receptor			Interaction	Distance	E (kcal/mol)
CL1	1	CG1 VAL	152	(B)	H-donor	3.38	-0.5
N1	5	OE1 GLU	172	(B)	H-donor	2.7	-9.5
N1	5	OE2 GLU	172	(B)	H-donor	3.16	-5.3
C3	8	OE2 GLU	172	(B)	H-donor	3.12	-1
C6	11	CD2 LEU	105	(B)	H-donor	4.16	-0.6
C8	13	CG1 VAL	84	(B)	H-donor	4.04	-0.5
C12	17	CE2 PHE	133	(B)	H-donor	3.65	-0.5
C18	23	CE MET	93	(B)	H-donor	3.89	-0.7
C18	23	CD1 LEU	95	(B)	H-donor	4.03	-0.5
C18	23	CD2 LEU	105	(B)	H-donor	4.01	-0.5
C19	24	CG2 ILE	178	(B)	H-donor	3.59	-0.8
C20	25	CD1 LEU	95	(B)	H-donor	3.82	-0.6
C20	25	CD2 LEU	95	(B)	H-donor	4.27	-0.5
CL1	1	CG1 VAL	152	(B)	H-acceptor	3.38	-0.5
C6	11	CD2 LEU	105	(B)	H-acceptor	4.16	-0.6
C8	13	CG1 VAL	84	(B)	H-acceptor	4.04	-0.5
C12	17	CE2 PHE	133	(B)	H-acceptor	3.65	-0.5
C18	23	CE MET	93	(B)	H-acceptor	3.89	-0.7
C18	23	CD1 LEU	95	(B)	H-acceptor	4.03	-0.5
C18	23	CD2 LEU	105	(B)	H-acceptor	4.01	-0.5
C19	24	CG2 ILE	178	(B)	H-acceptor	3.59	-0.8
C20	25	CD1 LEU	95	(B)	H-acceptor	3.82	-0.6
C20	25	CD2 LEU	95	(B)	H-acceptor	4.27	-0.5
N1	5	OE1 GLU	172	(B)	ionic	2.7	-6.8
N1	5	OE2 GLU	172	(B)	ionic	3.16	-3.5
C5	10	6-ring PHE	107	(B)	H-pi	4.37	-0.6
C13	18	5-ring HIS	154	(B)	H-pi	3.67	-1

Supplementary Table 3. Docking scores of Haloperidol in complex with Sigma receptor. Glide and Emodel docking scores obtained for the 18 docking experiments performed on the two crystal structures available for Sigmar1 (5HK1 and 5HK2, in yellow).

Monomer	Glide score	Emodel score
5HK1 chain A Halo conf. A	-9.686	-68.204
5HK1 chain A Halo conf. B	-9.024	-67.405
5HK1 chain A Halo conf. C	-6.506	-59.422
5HK1 chain B Halo conf. A	-10.619	-83.33
5HK1 chain B Halo conf. B	-8.501	-62.945
5HK1 chain B Halo conf. C	-7.062	-63.042
5HK1 chain C Halo conf. A	-10.298	-75.324
5HK1 chain C Halo conf. B	-8.767	-65.409
5HK1 chain C Halo conf. C	-4.832	-53.866
5HK2 chain A Halo conf. A	-10.396	-79.338
5HK2 chain A Halo conf. B	-8.059	-39.877
5HK2 chain A Halo conf. C	-6.701	-68.392
5HK2 chain B Halo conf. A	-10.745	-77.68
5HK2 chain B Halo conf. B	-8.198	-62.657
5HK2 chain B Halo conf. C	-6.356	-63.02
5HK2 chain C Halo conf. A	-10.128	-78.529
5HK2 chain C Halo conf. B	-9.081	-67.28
5HK2 chain C Halo conf. C	-5.471	-44.825

Supplementary Table 4. Detected binding sites with site score, size and volume.

Title	SiteScore	size	volume
5HK1_site_1	1.258	181	254.506
5HK1_site_2	1.233	160	223.293
5HK1_site_3	1.239	161	242.158
5HK1_site_4	1.168	185	284.004
5HK1_site_5	1.063	107	263.081
5HK2_site_2	1.285	184	245.245
5HK2_site_3	1.265	152	231.182
5HK2_site_1	1.258	191	247.646
5HK2_site_4	1.164	185	300.468
5HK2_site_5	1.016	89	265.139

Supplementary Table 5. List of primers with sequences.

Gene	Forward sequence	Reverse sequence
Chop/ Ddit3	ACCACACCTGAAAGCAGAAC	TCTTCCTCTTCGTTTCCTGG
Grp94 / Hsp90b	AGCACATCTGGGAATCAGAC	TGCTACTCCACACGTAGATG
Grp78 / Hspa5	GTTCTTCAATGGCAAGGAGC	TGAGACTTCTTGGTGGGTAC
p58 IpK / Dnajc3	GTGGAGTAAATGCGGATGTG	CAATCACTTTGGTGAGGTCG
Fkbp11	AGAAACCGAAAGTCCTGTCC	TTTGGCCGAGTTCTATGACC
Atf4	ATGGCCGGCTATGGATGAT	TCATCCAACGTGGTCAAGAG
Atf3	CGCCATCCAGAATAAACACC	TATTTCTTTCTCGCCGCCTC
Ccnd1	AGATGTGCCATCCATGC	CGGATGGTCTGCTTGTTC
Hes1	GCACCTCCGGAACCTGCAGCG	GCAGCCGAGTGCGCACCTCGG
Hey1	AAAGACGGAGAGGCATCATCG	GCAGTGTGAAGCATTTTCAGG
Notch1	GATGGCCTCAATGGGTACAAG	TCGTTGTTGTTGATGTCACAGT
Gadph	CGACTTCAACAGCAACTCCCACTCTTCC	TGGGTGGTCCAGGGTTTCTTACTCCTT
Sigmar1	GACAGTATGCGGGGCTGGACCA	CCAGTATCGTCCCGAATGGCCATG
Acta2	GGACGTACAACTGGTATTGTGC	TCGGCAGTAGTCACGAAGGA
Drd2	ATCTCTTGCCCACTGCTCTTTGGA	ATAGACCAGCAGGGTGACGATGAA
Col1a1	GCCAAGAAGACATCCCTGAAG	TCCGGGCAGAAAGCACAGCACT
Fn1	ATGTGGACCCCTCCTGATAGT	GCCCAGTGATTTCAGCAAAGG
Postn	CACGGCATGGTTATTCCTTC	TCAGGACACGGTCAATGACAT
Gadd34/ Ppp1r15a	GAGGGACGCCCACAACTTC	TTACCAGAGACAGGGGTAGGT

Supplementary Movie 1. Live imaging of Fluo4 fluorescence in primary adult cardiac fibroblasts treated Haloperidol. Cells were loaded with Fluo4 (green) and imaged by confocal microscopy for 20 seconds. Haloperidol was added at the indicated time in the movie.

Supplementary Movie 2. Live imaging of Fluo4 fluorescence in adult human dermal fibroblasts treated Haloperidol. Cells were loaded with Fluo4 (green) and imaged by confocal microscopy for 50 seconds. Haloperidol was added at the indicated time in the movie.